*Journal of Physiology* (2002), **545.2**, *pp.* 355–373
DOI: 10.1113/jphysiol.2002.032151

www.jphysiol.org



# Gating properties of GIRK channels activated by $G\alpha_o$- and $G\alpha_i$-coupled muscarinic m2 receptors in *Xenopus* oocytes: the role of receptor precoupling in RGS modulation

Qingli Zhang, Mary A. Pacheco* and Craig A. Doupnik

*Department of Physiology and Biophysics and *Department of Pharmacology and Therapeutics, University of South Florida College of Medicine, Tampa, Florida 33612-4799, USA*

**'Regulators of G protein Signalling' (RGSs) accelerate the activation and deactivation kinetics of G protein-gated inwardly rectifying $K^+$ (GIRK) channels. In an apparent paradox, RGSs do not reduce steady-state GIRK current amplitudes as expected from the accelerated rate of deactivation when reconstituted in *Xenopus* oocytes. We present evidence here that this kinetic anomaly is dependent on the degree of G protein-coupled receptor (GPCR) precoupling, which varies with different $G\alpha_{i/o}$–RGS complexes. The gating properties of GIRK channels (Kir3.1/Kir3.2a) activated by muscarinic m2 receptors at varying levels of G protein expression were examined with or without the co-expression of either RGS4 or RGS7 in *Xenopus* oocytes. Different levels of specific m2 receptor–$G\alpha$ coupling were established by uncoupling endogenous pertussis toxin (PTX)-sensitive $G\alpha_{i/o}$ subunits with PTX, while expressing varying amounts of a single PTX-insensitive subunit ($G\alpha_{i1(C351G)}$, $G\alpha_{i2(C352G)}$, $G\alpha_{i3(C351G)}$, $G\alpha_{oA(C351G)}$, or $G\alpha_{oB(C351G)}$). Co-expression of each of the PTX-insensitive $G\alpha_{i/o}$ subunits rescued acetylcholine (ACh)-elicited GIRK currents ($I_{K,ACh}$) in a concentration-dependent manner, with $G\alpha_o$ isoforms being more effective than $G\alpha_i$ isoforms. Receptor-independent 'basal' GIRK currents ($I_{K,basal}$) were reduced with increasing expression of PTX-insensitive $G\alpha$ subunits and were accompanied by a parallel rise in $I_{K,ACh}$. These effects together are indicative of increased $G\beta\gamma$ scavenging by the expressed $G\alpha$ subunit and the subsequent formation of functionally coupled m2 receptor-G protein heterotrimers ($G\alpha_{(GDP)}\beta\gamma$). Co-expression of RGS4 accelerated all the PTX-insensitive $G\alpha_{i/o}$-coupled GIRK currents to a similar extent, yet reduced $I_{K,ACh}$ amplitudes 60–90 % under conditions of low $G\alpha_{i/o}$ coupling. Kinetic analysis indicated the RGS4-dependent reduction in steady-state GIRK current was fully explained by the accelerated deactivation rate. Thus kinetic inconsistencies associated with RGS4-accelerated GIRK currents occur at a critical threshold of G protein coupling. In contrast to RGS4, RGS7 selectively accelerated $G\alpha_o$-coupled GIRK currents. Co-expression of $G\beta5$, in addition to enhancing the kinetic effects of RGS7, caused a significant reduction (70–85 %) in steady-state GIRK currents indicating RGS7–$G\beta5$ complexes disrupt $G\alpha_o$ coupling. Altogether these results provide further evidence for a GPCR–$G\alpha\beta\gamma$–GIRK signalling complex that is revealed by the modulatory affects of RGS proteins on GIRK channel gating. Our functional experiments demonstrate that the formation of this signalling complex is markedly dependent on the concentration and composition of G protein–RGS complexes.**

(Resubmitted 6 September 2002; accepted 16 September 2002; first published online 4 October 2002)
**Corresponding author** C. A. Doupnik: Department of Physiology and Biophysics, University of South Florida College of Medicine, 12901 Bruce B. Downs Blvd/MDC 8, Tampa, FL 33612-4799, USA. Email: cdoupnik@hsc.usf.edu

G protein-gated inwardly rectifying $K^+$ (GIRK) channels mediate slow inhibitory post-synaptic potentials (sIPSPs) in the central and peripheral nervous system and are activated by a variety of G protein-coupled receptors (GPCRs) that selectively interact with pertussis toxin (PTX)-sensitive $G\alpha_{i/o}$ proteins (for recent reviews see (Dascal, 1997; Yamada *et al.* 1998; Mark & Herlitze, 2000). Both the amplitude and the distinguishing slow time course for GIRK-mediated sIPSPs are inherently coupled to the kinetics of the G protein activation–deactivation cycle. The time course for GIRK channel activation is dependent on the receptor catalysed production of free $G\beta\gamma$ dimers that interact directly with the channel and increase open probability (Logothetis *et al.* 1987; Krapivinsky *et al.* 1995). Deactivation of GIRK currents is determined by the reaction rate for $G\beta\gamma$ sequestration, a process rate limited by the GTPase activity of associated $G\alpha_{i/o}$ proteins, $G\alpha_{(GTP)} \rightarrow G\alpha_{(GDP)}$, with a rate constant for GTP hydrolysis of $k_{GTPase}$ (Breitwieser & Szabo, 1988).

**Table 1. Heterologously expressed proteins in *Xenopus* oocytes**

| cDNA | GenBank accession # | Cloning vector |
|---|---|---|
| Human muscarinic m2 receptor | X15264 | pGEM3 (Promega) |
| Rat Kir3.1 | U01071 | pBS-MXT* |
| Mouse Kir3.2a | U37253 | pBS-MXT* |
| Rat $G\alpha_{i1(C351G)}$ | M17527 | pCI (Promega) |
| Rat $G\alpha_{i2(C352G)}$ | M17528 | pCI (Promega) |
| Rat $G\alpha_{i3(C351G)}$ | M20713 | pCI (Promega) |
| Mouse $G\alpha_{oA(C351G)}$ | M36777 | pCI (Promega) |
| Mouse $G\alpha_{oB(C351G)}$ | M36778 | pCI (Promega) |
| Bovine $G\beta1$ | M13236 | pBS-MXT* |
| Mouse $G\beta5$ | U69145 | pcDNA3 (Invitrogen) |
| Rat RGS4 | U27767 | pcDNA3.1 (Invitrogen) |
| Bovine RGS7 | AF011359 | pcDNA3 (Invitrogen) |
| PTX-S1 | M13223 | pGEMHE* |

* The pBS-MXT and pGEMHE vectors are modified pBluescript II (KS) (Stratagene) and PGEM-3Z (Promega) vectors, each containing 5′ and 3′ untranslated regions of the *Xenopus* $\beta$-globin gene that flank the cloned cDNA and enhance RNA stability in *Xenopus* oocytes (Liman *et al.* 1992).

Given the large diversity and ubiquitous expression of heterotrimeric G proteins (Simon *et al.* 1991), several studies have begun investigating whether functional differences exist among the various $G\alpha\beta\gamma$ subunits that may participate in GPCR → GIRK channel signalling (5 $G\alpha_{i/o}$ isoforms, 5 $G\beta$ genes, and 12 $G\gamma$ genes) (Lledo *et al.* 1992; Wickman *et al.* 1994; Schreibmayer *et al.* 1996; Sowell *et al.* 1997; Takano *et al.* 1997; Valenzuela *et al.* 1997; Fernandez-Fernandez *et al.* 1999; Greif *et al.* 2000; Leaney *et al.* 2000; Leaney & Tinker, 2000; Lei *et al.* 2000; Blake *et al.* 2001; Fernandez-Fernandez *et al.* 2001). Adding to this molecular complexity is the recently identified 'Regulators of G protein Signalling' (RGSs) that accelerate the termination of G protein signalling by increasing $k_{GTPase}$ through a direct interaction with $G\alpha$ subunits (for recent reviews see De Vries *et al.* 2000; Ross & Wilkie, 2000). Several RGS proteins, of which there are now more than 20 mammalian genes identified, are capable of accelerating receptor-dependent GIRK activation and deactivation kinetics in heterologous expression systems (Doupnik *et al.* 1997; Saitoh *et al.* 1997; Granneman *et al.* 1998; Herlitze *et al.* 1999; Saitoh *et al.* 1999; Kovoor *et al.* 2000; Burgon *et al.* 2001). RGS-accelerated GIRK currents more closely resemble the properties of neuronal and cardiac GIRK currents, indicating native RGS proteins are likely to be important determinants of GIRK-mediated synaptic signalling.

Initial studies of RGS-accelerated GIRK channel kinetics revealed an apparent paradox where the RGS-accelerated activation phase, an expected consequence of accelerated deactivation according to standard kinetic concepts, was not accompanied with a reduction in steady-state current amplitude (Doupnik *et al.* 1997; Saitoh *et al.* 1997). These findings suggested that RGS proteins have actions on GPCR → GIRK signalling beyond the well-established GTPase-activating function of the RGS domain on $G\alpha_{(GTP)}$ subunits (Zerangue & Jan, 1998). To further explore the effects of RGS proteins on receptor-dependent GIRK channel gating, we examined the actions of two distinct RGS proteins (RGS4 and RGS7) on GIRK channels (Kir3.1/Kir3.2a heteromers) activated by muscarinic m2 receptors coupled to varying concentrations and compositions of $G\alpha_{i/o}\beta\gamma$ heterotrimers in *Xenopus* oocytes. Muscarinic m2 receptor–$G\alpha\beta\gamma$–GIRK channel coupling was established by expressing varying levels of PTX-insensitive $G\alpha_{i/o}$ subunits (Wise *et al.* 1997) while uncoupling oocyte $G\alpha_{i/o}$ subunits ($xG\alpha_{i/o}$) with PTX. Our findings indicate that GPCR–G protein–RGS–GIRK precoupling is a critical determinant in the anomalous channel gating, and is dependent on the concentration and composition of $G\alpha_{i/o}$–RGS proteins.

## METHODS

### Isolation of *Xenopus* oocytes

All procedures for the use and handling of *Xenopus laevis* (Xenopus One, Ann Arbor, MI, USA) were approved by the University of South Florida Institutional Animal Care and Use Committee in accordance with NIH guidelines. Oocytes were isolated from ovarian tissue surgically removed during hypothermia and 0.2% tricaine (MS-222)-induced anaesthesia. After recovery from anaesthesia, frogs were returned to their tanks in the institutional animal housing facility where they were monitored daily. Frogs were killed after a second procedure by exsanguination while under anaesthesia. The time between surgeries was 1–3 weeks.

The oocytes were enzymatically dissociated by a 50 min collagenase A (Boehringer Mannheim) digestion (1.8 %) at room temperature on a rocker platform in $Ca^{2+}$-free oocyte Ringer (OR) solution. The OR solution was composed of 82.5 mM NaCl, 2.5 mM KCl, 1.0 mM $CaCl_2$, 1.0 mM $MgCl_2$, 1.0 mM $NaHPO_4$ and 5.0 mM Hepes, at pH 7.5 (NaOH). Isolated stage V–VI oocytes were then maintained in oocyte culture medium (OCM) at 19 °C in 35 mm dishes on an orbital shaker. OCM was composed of OR solution containing 2.5 mM sodium pyruvate and 5 % heat-inactivated horse serum. OCM was changed 1–2 times daily.

### Heterologous expression in *Xenopus* oocytes

Linearized cDNA-containing vectors (Table 1) were used to transcribe cRNA *in vitro* using the appropriate RNA polymerase (T7 or T3) as described by the manufacturer (mMessage mMachine, Ambion, Austin, TX, USA). Concentrations and quality of the cRNAs were determined by spectrophotometric absorbance at 260 nm and denatured (formaldehyde) agarose gel electrophoresis. On the first day after enzymatic isolation (Day 1), oocytes were injected with a mixture of cRNAs dissolved in DEPC-treated $H_2O$ at a final injection volume of 50 nl (Nanoliter2000, World Precision Instruments). All oocytes were injected with cRNAs for Kir3.1 (0.5 ng), Kir3.2a (0.5 ng), and the m2 receptor (0.5 ng). The amounts of other cRNAs, including PTX-insensitive $G\alpha$ subunits and RGSs, were varied as described in the Results section. The PTX-insensitive $G\alpha$ cDNAs were all constructed by PCR (kindly provided by Stephen Ikeda, NIAAA,

Bethesda, MD, USA), having a 5′ Kozak sequence followed by the Gα coding region containing the C-terminal C→G mutation. The 5′ and 3′ untranslated regions of the Gα cDNAs were not included in the constructs, and therefore ribosomal binding and translation initiation of each PTX-insensitive Gα cRNA are expected to be equivalent.

Two methods were used to inactivate endogenous oocyte $G\alpha_{i/o}$ subunits by PTX-mediated ADP ribosylation. Initially we injected the PTX holotoxin (containing S1, S2, S3, S4 and S5 subunits from *Bordetella pertussis*, Sigma-Aldrich Chemical) at 1 ng/oocyte on Day 2 of culture (1 day after cRNA injection), and then recorded GIRK currents on Day 4. This method inhibited > 80 % of the m2 receptor-activated GIRK currents coupled to endogenous $G\alpha_{i/o}$ subunits that was determined for each batch of oocytes to monitor the efficiency of endogenous G protein uncoupling. In subsequent experiments we included cRNA (1 ng/oocyte) encoding the catalytically active PTX-S1 subunit (kindly provided by Eitan Reuveny, Weizmann Institute, Israel) with the mixture of other cRNAs in the initial Day 1 cRNA injection (Vivaudou *et al.* 1997). This produced a much more effective > 95 % uncoupling of endogenous $G\alpha_{i/o}$ subunits which also was determined for each batch of oocytes tested.

**Electrophysiological recordings**

Macroscopic GIRK currents were measured using a two-electrode voltage clamp amplifier (GeneClamp 500, Axon Instruments) and standard recording techniques (Stuhmer & Parekh, 1995). Electrodes were fabricated from borosilicate glass tubes (1.5 outside diameter, 0.86 inside diameter, GC150F-10, Warner Instruments) by a programmable microelectrode puller (P-97, Sutter Instruments). Electrodes were filled with 3 M KCl and had tip resistances of 0.8–1.0 MΩ. Membrane currents from voltage clamped oocytes were digitized using a Digidata 1200 acquisition system (Axon Instruments) and a Dell PC computer running pCLAMP 7.0 software (Axon Instruments).

Oocytes were placed in a recording chamber continuously perfused with a minimal Ringer solution composed of 98 mM NaCl, 1 mM $MgCl_2$ and 5 mM Hepes at pH 7.5 (NaOH). After electrode impalement and clamping the membrane potential to −80 mV, the perfusion solution was changed to a high $K^+$ solution composed of 20 mM KCl, 78 mM NaCl, 1 mM $MgCl_2$, and 5 mM Hepes at pH 7.5 (NaOH). The resulting increase in inward current represents a 'basal' $K^+$ current ($I_{K,basal}$) that is due primarily to receptor-independent GIRK channel activity (Dascal *et al.* 1993). Rapid application and washout of acetylcholine (ACh, Sigma-Aldrich Chemical) produced the receptor-dependent GIRK current ($I_{K,ACh}$), and was performed with a computer controlled perfusion system (SF-77B, Warner Instruments) that rapidly switched the position of two perfusion barrels (barrel A and barrel B) located next to the oocyte. The perfusion barrels contained high $K^+$ solution (barrel A) and high $K^+$ solution plus ACh (barrel B). For barrel B, a range of ACh concentrations was tested for each oocyte via a manifold that connected multiple reservoirs containing different ACh concentrations. Flow through the perfusion barrels was gravity driven, and the time constant for solution exchange was ~1 s as determined by the time course change in receptor-independent GIRK current with switching between 20 and 40 mM external $K^+$. All recordings were performed at room temperature (21–23 °C).

**Electrophysiological data analysis**

Time-dependent GIRK current kinetics were analysed using non-linear curve fitting software that fit single exponential functions to derive activation time constants ($\tau_{act}$) and deactivation time constants ($\tau_{deact}$) (Clampfit software, Axon Instruments). Dose–response relations were analysed by fitting peak GIRK current amplitudes with the following Hill function:

$$\frac{I_{K,ACh}}{I_{Max}} = \frac{1}{1 + \left(\frac{[ACh]}{EC_{50}}\right)^{n_H}},$$

where the effective concentration producing a 50 % response ($EC_{50}$) and Hill coefficient value ($n_H$) were derived from the best fit (Origin 6.0 software, OriginLab Corp., Northampton, MA, USA). In some cases where the GIRK current did not reach a steady-state level at the end of the agonist application period (i.e. low agonist concentrations), the steady-state current amplitude was estimated by the fit of the activation time course to an extrapolated steady-state value.

Statistical comparisons between the various experimental groups were performed by one-way ANOVA where $P < 0.05$ was considered significant. Experiments were each replicated in oocytes from 2–4 separate batches (dissections) of oocytes.

**Radiolabelling, immunoprecipitation and Western blotting of $G\alpha_{i/o}$ proteins**

To compare the relative expression levels of PTX-insensitive $G\alpha_{i/o}$ proteins, [$^{35}$S]Met/Cys (Pro-mix, Amersham Pharmacia, Piscataway, NJ, USA) was added to OCM (0.5 mCi ml$^{-1}$) 1–2 h after cRNA injection to initiate radiolabelling of proteins. Fresh OCM containing [$^{35}$S]Met/Cys was added on a daily basis, and 3 days after cRNA injection ~20 oocytes from each experimental group were washed with label-free OR solution and homogenized in the following lysis buffer (150 mM NaCl, 50 mM Tris-Cl, 1 mM dithiothreitol (DTT), 1.0 % Trition X-100, and protease inhibitor cocktail (Boehringer Mannheim), pH 7.5) at 50 μl/oocyte. The oocyte lysate was then centrifuged at 10 000 *g* for 10 min to clear insoluble debris.

$G\alpha_{i/o}$ subunits were immunoprecipitated from oocyte lysates using a rabbit polyclonal antibody that recognizes an internal epitope (GAGESGKSTIVKQMK) identical among $G\alpha_{i/o}$ isoforms (SA-126, BIOMOL Research Laboratories, Plymouth Meeting, PA, USA). To expose the internal epitope, the supernatant from the equivalent of five oocytes (250 μl) was diluted in SDS denaturing buffer (50 mM $NaPO_4$, 2 mM EDTA, 1 mM DTT, 0.5 % SDS, pH 8.0) and boiled for 3 min. The denaturated supernatants were then diluted and solubilized further in RIPA buffer (150 mM NaCl, 50 mM $NaPO_4$, 2 mM EDTA, 1 mM DTT, 1.0 % Triton X-100, 1.0 % deoxycholate, 0.5 % SDS, pH 7.2). Denatured oocyte lysates (~700 μl each) were then pre-cleared with 10 μl of non-immune rabbit serum (1 h incubation at 4 °C) and 20 μl Protein A/G–agarose beads (Santa Cruz Biotechnology, Inc.). $G\alpha_{i/o}$ proteins were immunoprecipitated in an overnight incubation at 4 °C using the SA-126 antibody precoupled to Protein A/G–agarose beads. We initially tested different amounts of oocyte lysate (0.5, 1, 2 and 4 oocytes) with a fixed amount of SA-126 antibody (2 μl) and Protein A/G–agarose (20 μl) to establish non-saturating binding conditions, which was determined to be ⩽ 1 oocyte. All immunoprecipitations were then performed using the lysate equivalent of a single oocyte. At the end of the overnight incubation period, beads were washed three times with lysis buffer and the immunoprecipitated proteins eluted by boiling in 40 μl of SDS loading buffer (62.5 mM Tris-Cl pH 6.8, 10 % glycerol, 5 % β-mercaptoethanol, 2 % SDS, 0.05 % bromophenol blue).

Journal of Physiology

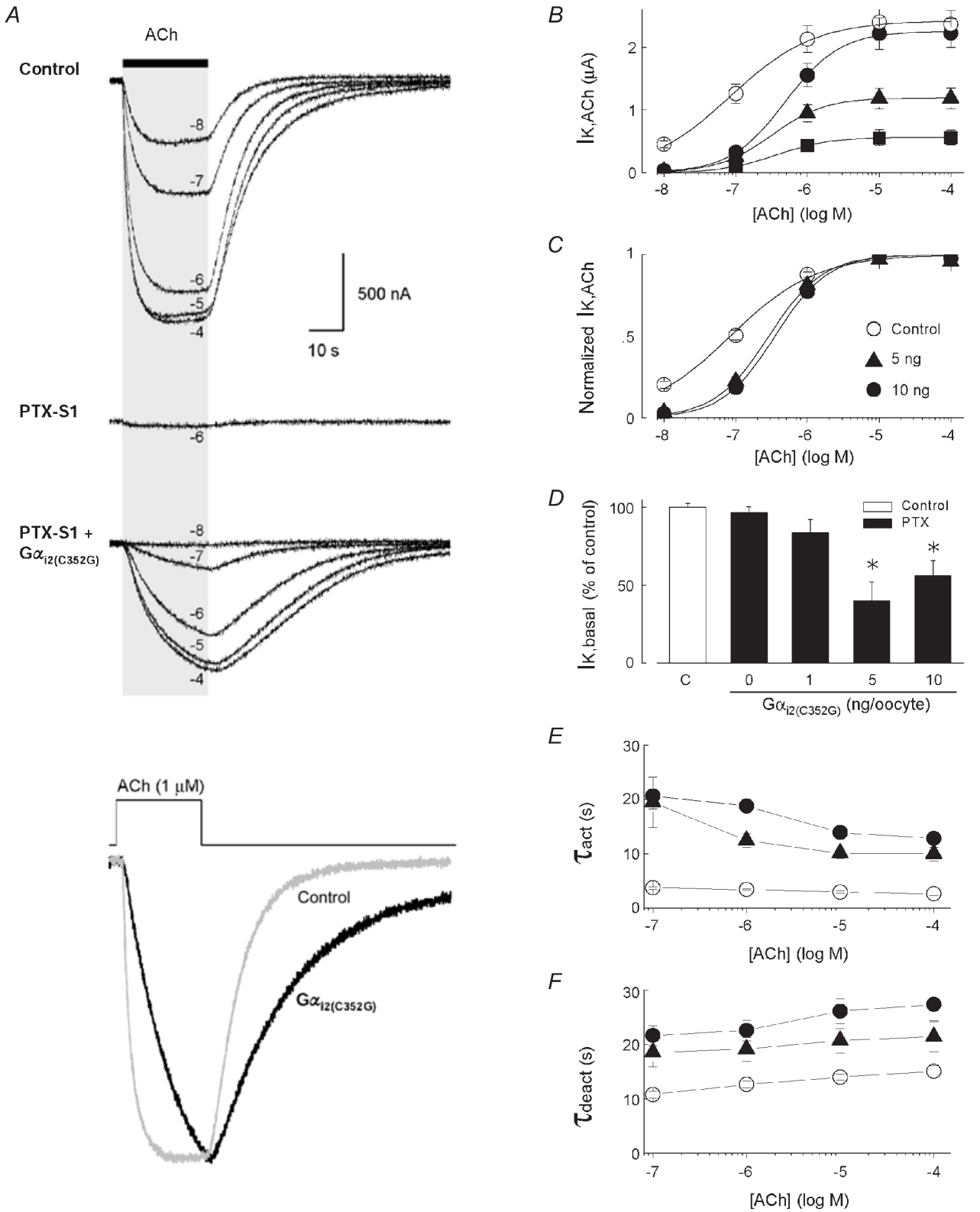


**Figure 1. Specific coupling of $G\alpha_{i2(C352G)}$ to m2 receptors and GIRK channel activation in *Xenopus* oocytes**

*A*, typical ACh-evoked GIRK currents ($I_{K,ACh}$) recorded from different oocytes from three separate experimental groups. Upper traces: $I_{K,ACh}$ from a 'control' oocyte expressing muscarinic m2 receptors and Kir3.1/Kir3.2a channel subunits, utilizing endogenous $G\alpha_{i/o}$ proteins for receptor activation. Middle trace: co-expression of PTX-S1 (1 ng cRNA/oocyte) effectively uncouples ACh-evoked GIRK currents utilizing oocyte $G\alpha_{i/o}$ proteins. Lower traces: expression of the PTX-insensitive $G\alpha_{i2(C352G)}$ subunit (5 ng cRNA) with PTX-S1 rescues m2 receptor-coupled GIRK currents. All GIRK currents were elicited by a 25 s application of

Immunoprecipitated proteins were separated by SDS–polyacrylamide (8%) gel electrophoresis and then transferred to a polyvinylidene difluoride (PVDF) membrane by overnight electrophoretic transfer at 4°C. $^{35}$S–labelled proteins were resolved by autoradiography. Western blot analysis was performed using a polyclonal goat antibody that recognizes a conserved region in $G\alpha_{i/o/t/z}$ proteins (sc-12798, Santa Cruz Biotechnology). A ~41 kDa band corresponding to $G\alpha_{i/o}$ proteins was readily detected by an HRP-conjugated donkey anti-goat secondary antibody (sc-2033, Santa Cruz Biotechnology) and enhanced chemiluminescence. Relative radiolabelling and $G\alpha_{i/o}$ protein levels were quantified by densitometric analysis (GS-700 Imaging Densitometer, Bio-Rad) of the 41 kDa band following normalization to a sample control.

## RESULTS

### Conferring specific m2 receptor–Gα-coupling in *Xenopus* oocytes

To assess the properties of receptor-dependent GIRK channel gating elicited by specific Gα-coupled m2 receptors, oocyte $G\alpha_{i/o}$ subunits were inactivated by PTX while expressing one of five different PTX-insensitive $G\alpha_{i/o}$ subunits ($G\alpha_{i1(C351G)}$, $G\alpha_{i2(C352G)}$, $G\alpha_{i3(C351G)}$, $G\alpha_{oA(C351G)}$, or $G\alpha_{oB(C351G)}$) (Wise *et al.* 1997). As reported previously, expression of PTX-S1 blocked > 95% of $I_{K,ACh}$ and effectively abolished endogenous $G\alpha_{i/o}$ protein coupling (Vivaudou *et al.* 1997). Shown in Fig. 1, co-expression of $G\alpha_{i2(C352G)}$ rescued the m2 receptor-coupled GIRK currents and was dependent on the level of $G\alpha_{i2(C352G)}$ expression (Fig. 1*B*). Injection of 5 or 10 ng of $G\alpha_{i2(C352G)}$ cRNA per oocyte produced ACh-evoked GIRK currents that were ~50 and 95%, respectively, the peak amplitude of GIRK currents recorded from paired oocytes utilizing endogenous $G\alpha_{i/o}$ subunits (i.e. no PTX-S1 or $G\alpha_{i2(C352G)}$ cRNA). The $G\alpha_{i2(C352G)}$-dependent GIRK currents represent channels activated by m2 receptors coupled specifically to $G\alpha_{i2(C352G)}$ subunits and endogenous $G\beta\gamma$ dimers. $G\alpha_{i2(C352G)}$-dependent $I_{K,ACh}$ was also associated with a parallel 50–60% *decrease* in $I_{K,basal}$ (Fig. 1*D*). The reduction in $I_{K,basal}$ by $G\alpha_{i2(C352G)}$ is likely due to the sequestration of free $G\beta\gamma$ dimers that mediate receptor-independent basal GIRK channel activity (Lim *et al.* 1995; Vivaudou *et al.* 1997; Jeong & Ikeda, 1999).

ACh dose–response curves derived from oocytes expressing different levels of $G\alpha_{i2(C352G)}$ were not significantly different with respect to their $EC_{50}$ value as shown in Fig. 1*C*, and this is consistent with previous studies where $EC_{50}$ values were shown to be relatively unaffected by overexpressed Gα subunits, but most sensitive to levels of GPCR expression (Henry *et al.* 1995). Since the same amount of m2 receptor cRNA was injected for all experimental groups (0.5 ng cRNA/oocyte), m2 receptor protein levels were assumed to be roughly equivalent across groups and this was supported by the equivalent $EC_{50}$ values with varying $G\alpha_{i2(C352G)}$ expression levels. The ACh dose–response curves for $G\alpha_{i2(C352G)}$-coupled m2 receptors, however, were notably shifted rightward compared to the ACh dose–response relation from m2 receptor coupling to endogenous $G\alpha_{i/o}$ subunits (Fig. 1*B*). The higher $EC_{50}$ value for $G\alpha_{i2(C352G)}$ *versus* endogenous $G\alpha_{i/o}$-coupled receptors may be attributable to the mixed coupling of oocyte $G\alpha_o$ and $G\alpha_i$ subunits, and/or a lower level of m2 receptors precoupled to heterotrimeric G proteins (Shea & Linderman, 1997; Shea *et al.* 2000) (see Results below and Discussion).

One readily apparent feature of the m2 receptor–$G\alpha_{i2(C352G)}$-coupled GIRK current was the significantly slower activation and deactivation kinetics as compared to GIRK currents coupled to endogenous x$G\alpha_{i/o}$ subunits (Fig. 1*A*). The time constants for $I_{K,ACh}$ activation and deactivation over a range of ACh concentrations are shown in Fig. 1*E* and *F*. The slower kinetics for m2 receptor–$G\alpha_{i2(C352G)}$-coupled GIRK currents were not attributable to the level of $G\alpha_{i2(C352G)}$ expression since increasing amounts of $G\alpha_{i2(C352G)}$ cRNA, which nearly doubled maximal $I_{K,ACh}$ amplitudes, did not result in significantly different GIRK activation or deactivation time constants. The slower GIRK gating properties may be caused by altered coupling properties of the C→G mutated $G\alpha_{i2}$ subunit, or alternatively the faster properties in the absence of overexpressed Gα subunits may reflect the influence of endogenous RGS proteins (Saitoh *et al.* 2000).

### GIRK channel gating properties via $G\alpha_o$- and $G\alpha_i$-coupled m2 receptors

The gating properties of GIRK currents elicited by m2 receptors coupled to each of the PTX-insensitive $G\alpha_{i/o}$ subunits are shown in Fig. 2. Since there were no noticeable differences in GIRK current kinetics at different

different concentrations of ACh as indicated. Bottom traces: superimposed $I_{K,ACh}$ elicited by 1 μM ACh from the control oocyte (grey trace) and the $G\alpha_{i2(C352G)}$-coupled oocyte (black trace). Peak amplitudes are normalized to illustrate the kinetic differences in the activation and deactivation time courses. *B*, ACh dose–response relations for GIRK activation via m2 receptors coupled to oocyte $G\alpha_{i/o}$ subunits (○, control) and $G\alpha_{i2(C352G)}$ at different levels of expression (■ 1 ng, ▲ 5 ng, and ● 10 ng cRNA/oocyte). *C*, ACh-dose–response curves from *B* normalized to maximal $I_{K,ACh}$. *D*, comparison of receptor-independent basal GIRK currents ($I_{K,basal}$) with varying levels of $G\alpha_{i2(C352G)}$ expression. $I_{K,basal}$ is expressed as the percentage change in the 'control group' mean value determined for each batch of oocytes. *E*, activation time constants ($\tau_{act}$) and *F*, deactivation time constants ($\tau_{deact}$) for GIRK currents coupled to varying levels of $G\alpha_{i2(C352G)}$ expression and different concentrations of ACh. ○ control; ▲ 5 ng; and ● 10 ng of $G\alpha_{i2(C352G)}$ cRNA/oocyte. Data in *B–F* represent the means ± S.E.M. from at least 3 batches of oocytes with the number of oocytes indicated. * $P < 0.05$.

Journal of Physiology

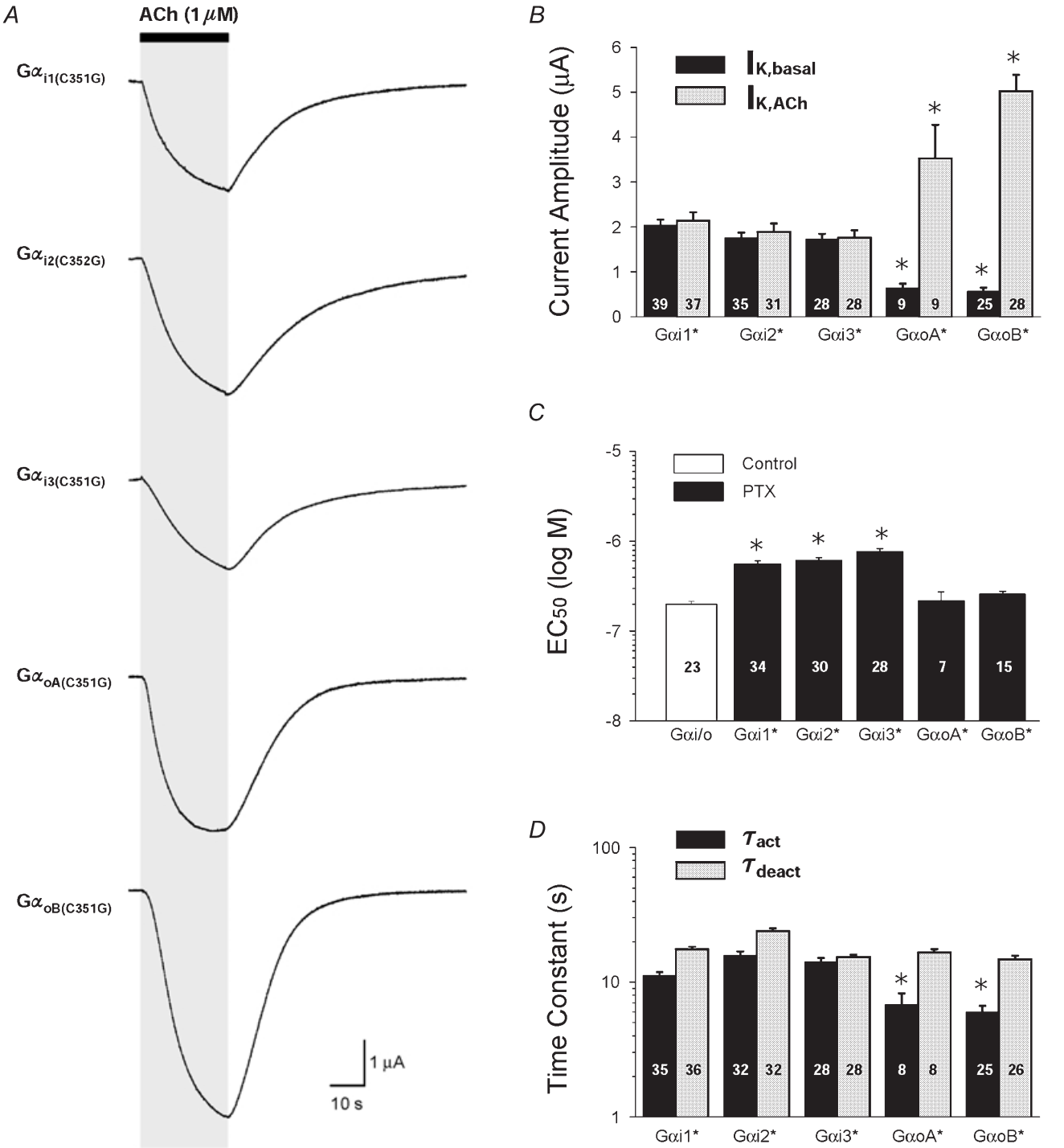


**Figure 2. Properties of ACh-evoked GIRK currents activated by m2 receptors coupled to five different G$\alpha_{i/o}$ subunits**

*A*, typical ACh-evoked GIRK currents for each PTX-insensitive G$\alpha_{i/o}$ subunit examined (G$\alpha_{i1(C351G)}$, G$\alpha_{i2(C352G)}$, G$\alpha_{i3(C351G)}$, G$\alpha_{oA(C351G)}$ and G$\alpha_{oB(C351G)}$). Currents were elicited by a 25 s application of 1 $\mu$M ACh. *B*, maximal amplitude of receptor-dependent GIRK currents ($I_{K,ACh}$, grey bars) and receptor-independent GIRK currents ($I_{K,basal}$, black bars) for each expressed PTX-insensitive G$\alpha$ subunit (G$\alpha^*$). G$\alpha^*$ expression was produced by 5 ng cRNA/oocyte. Maximal $I_{K,ACh}$ responses are to 10 $\mu$M ACh. *C*, $EC_{50}$ values for control (open bar) and each PTX-insensitive G$\alpha^*$ subunit, derived from ACh dose–response relations for $I_{K,ACh}$ activation. *D*, activation (black bars) and deactivation time constants (grey bars) derived from exponential fits of the $I_{K,ACh}$ time course in response to rapid ACh application and washout. For *B*–*D*, data represent the means + S.E.M. from at least 3 batches of oocytes with the number of oocytes indicated (*$P < 0.05$). In *B* and *D*, statistical comparisons were with G$\alpha_{i1(C351G)}$, and in *C* comparisons were with oocyte G$\alpha_{i/o}$ coupling (open bar).

levels of $G\alpha_{i2(C352G)}$ expression, comparisons between the five different $G\alpha_{i/o}$ isoforms were initially made using 5 ng cRNA/oocyte for each Gα isoform. The three $G\alpha_{i}$ isoforms ($G\alpha_{i1(C351G)}$, $G\alpha_{i2(C352G)}$ and $G\alpha_{i3(C351G)}$) each produced ACh-elicited GIRK currents that were indistinguishable from each other with regard to the five parameters analysed (maximal $I_{K,ACh}$, $I_{K,basal}$, $EC_{50}$, $\tau_{act}$ and $\tau_{deact}$) (Fig. 2). $G\alpha_{oA(C351G)}$ and $G\alpha_{oB(C351G)}$ also produced equivalent GIRK responses but were distinct from $G\alpha_{i}$-coupled GIRK currents in several respects. First, $G\alpha_{o}$-coupled GIRK currents were significantly larger than $G\alpha_{i}$-coupled currents, with maximal $I_{K,ACh}$ amplitudes being ~2-fold greater (Fig. 2*B*). Second, expression of $G\alpha_{oA(C351G)}$ and $G\alpha_{oB(C351G)}$ more prominently inhibited $I_{K,basal}$ compared to $G\alpha_{i1(C351G)}$, $G\alpha_{i2(C352G)}$, or $G\alpha_{i3(C351G)}$ (Fig. 2*B*). Third, the $EC_{50}$ values for $G\alpha_{oA(C351G)}$ and $G\alpha_{oB(C351G)}$ were more similar to the $EC_{50}$ values with endogenous $xG\alpha_{i/o}$ coupling than with $G\alpha_{i1(C351G)}$, $G\alpha_{i2(C352G)}$, or $G\alpha_{i3(C351G)}$ (Fig. 2*C*). And finally, the activation of $G\alpha_{o}$-coupled GIRK currents was faster compared to $G\alpha_{i}$-coupled currents and had a more prominent sigmoidal time course (Fig. 2*D*). The deactivation time course for $I_{K,ACh}$ was not significantly different among all five $G\alpha_{i/o}$ isoforms (Fig. 2*D*).

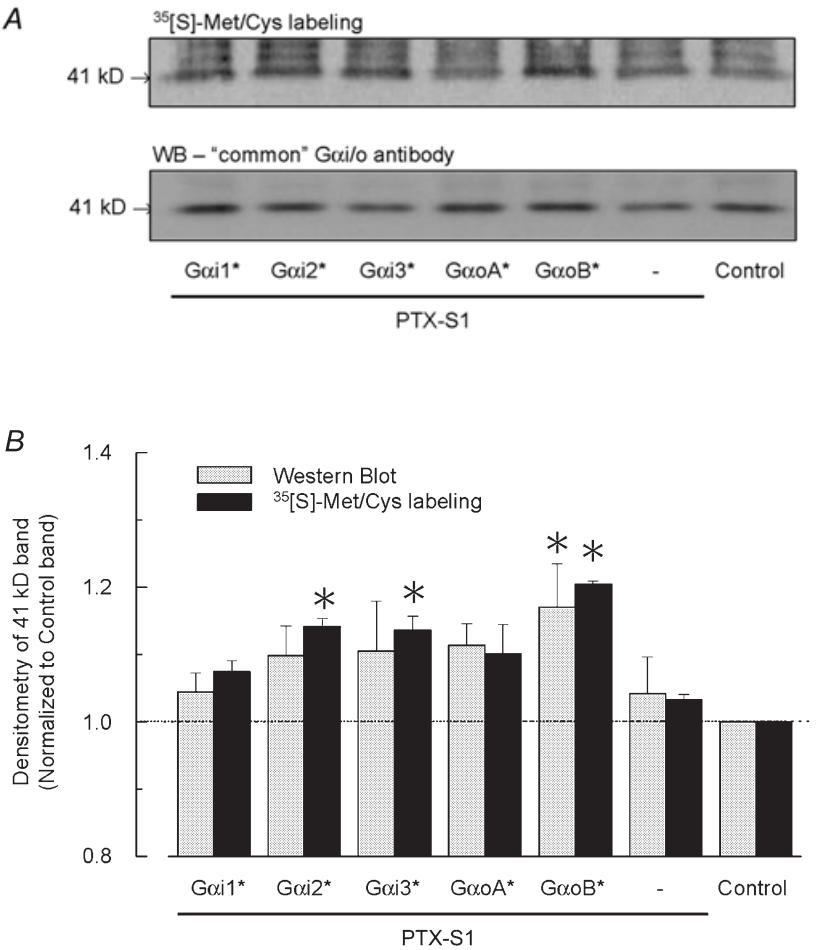


**Figure 3. Biochemical analysis of PTX-insensitive $G\alpha_{i/o}$ protein levels in *Xenopus* oocytes**

*A*, radiolabelling (upper panel) and Western blot analysis (lower panel) of oocytes injected with cRNAs encoding five different PTX-insensitive $G\alpha_{i/o}$ subunits (✱) as described in Methods and Fig. 2. Oocytes were incubated for 3 days in OCM containing 0.5 mCi $ml^{-1}$ [$^{35}$S]Met/Cys. All groups were injected with cRNAs for the m2 receptor and GIRK channel subunits Kir3.1 and Kir3.2a (0.5 ng each/oocyte). PTX-insensitive $G\alpha_{i/o}$ cRNAs (5 ng/oocyte) were injected with PTX-S1 cRNA (1 ng/oocyte). Both endogenous and heterologously expressed Gα proteins were immunoprecipitated from the lysate equivalent of one oocyte using a 'common' Gα antibody, then separated by SDS–PAGE and transferred to a PVDF membrane for autoradiography and Western blotting. The 41 kDa band corresponding to $G\alpha_{i/o}$ proteins is indicated. *B*, quantitative analysis of $G\alpha_{i/o}$ proteins detected by radiolabelling and Western blot analysis. The 41 kDa band from the control group (no PTX-insensitive $G\alpha_{i/o}$ cRNA) served as an internal reference and was used to normalize the band intensity among the different experimental groups in each autoradiogram and Western blot. The Western blot results are the means + S.E.M. obtained from 3 independent experiments (separate batches of injected oocytes that were immunoprecipitated and immunostained as described in Methods). The radiolabelling data are the means + S.E.M. obtained from 2 of the Western blot experiments. * $P < 0.05$.

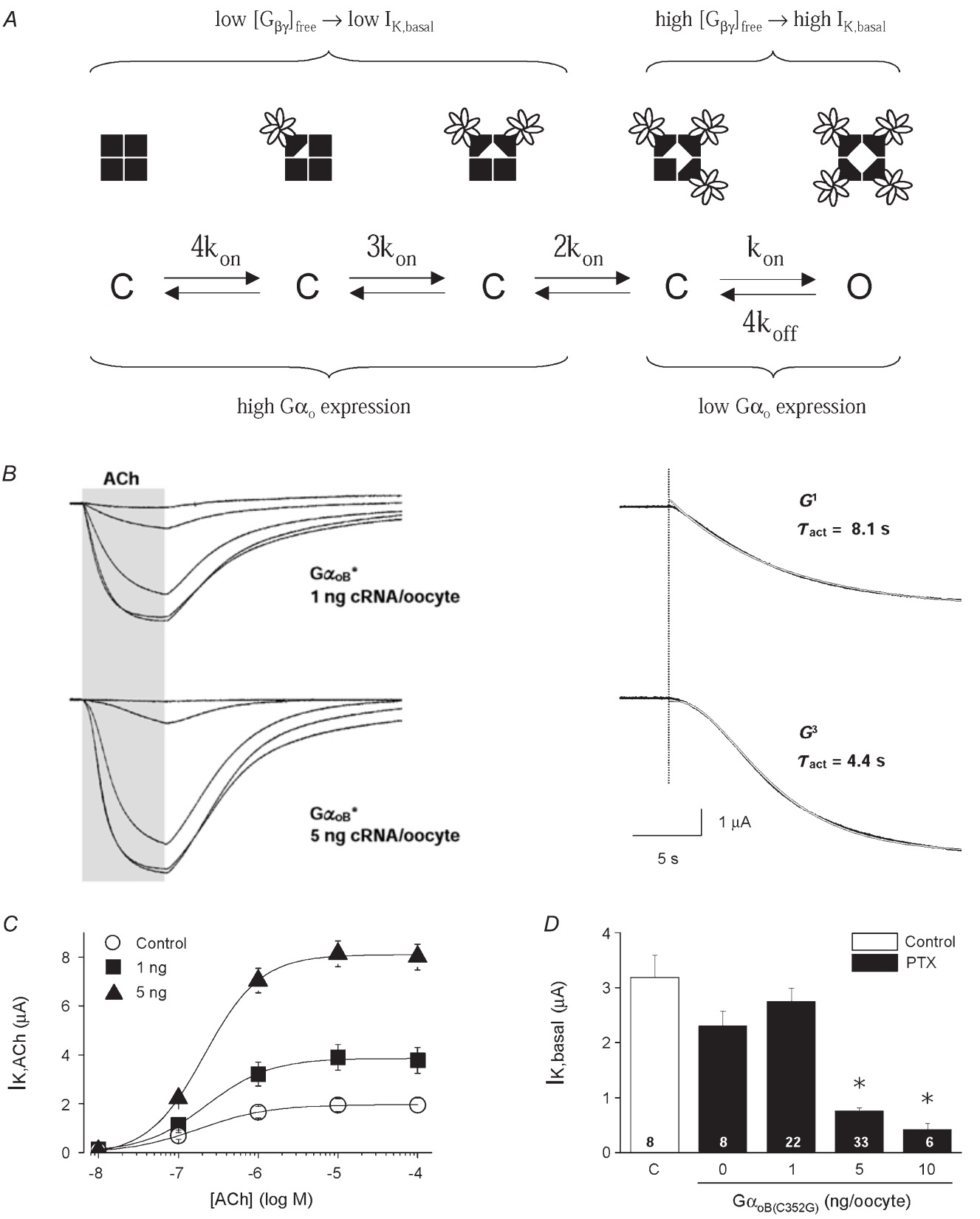


**Figure 4. Activation kinetics of $G\alpha_o$–coupled GIRK currents at different levels of $G\alpha_{oB(C352G)}$ expression**

*A*, kinetic scheme for GIRK channel activation via $G\beta\gamma$ binding to each of the four GIRK channel subunits. Four closed states are depicted with 0 to 3 bound $G\beta\gamma$ dimers. Channel opening (O) occurs with the binding of 4 $G\beta\gamma$ dimers. The level of free $G\beta\gamma$ dimers then determines the channel-bound state that precedes

The differences between $G\alpha_i$ and $G\alpha_o$-coupled GIRK currents were not attributable to cDNA/vector construction (i.e. untranslated regions), cRNA quantification, or batch-to-batch oocyte variability (see Methods). Several factors could conceivably contribute to these differences and include (1) differences in $G\alpha_{i/o}$ biosynthesis or degradation (Li *et al.* 1996), (2) preferential $G\alpha_o$ coupling to m2 receptors (Leaney & Tinker, 2000), (3) preferential $G\alpha_o$ association with oocyte $G\beta\gamma$ subunits (Fernandez-Fernandez *et al.* 2001), and (4) different $G\alpha_{i/o}$ subcellular distributions (Devic *et al.* 1996).

### Biochemical analysis of PTX-insensitive $G\alpha_{i/o}$ protein expression levels

To determine whether PTX-insensitive $G\alpha_{i/o}$ subunits are differentially expressed following cRNA injection (5 ng cRNA/oocyte, as in Fig. 2), $G\alpha_{i/o}$ proteins were immunoprecipitated from oocytes following metabolic labelling with [$^{35}$S]Met/Cys. The PTX-insensitive $G\alpha_{i/o}$ proteins each contain an equivalent number of Met/Cys sites (19) for potential radiolabelling. As shown in Fig. 3*A*, a prominent ~41 kDa band that corresponds to $G\alpha_{i/o}$ proteins was radiolabelled in each experimental group. A significant portion represents radiolabelling of endogenous x$G\alpha_{i/o}$ proteins over the 3 day incubation period as indicated by the oocyte groups that were not injected with PTX-insensitive $G\alpha_{i/o}$ cRNA. Quantitative comparisons of the $^{35}$S-labelled 41 kDa band via densitometric analysis indicate a small 10–20 % elevation in oocytes injected with PTX-insensitive $G\alpha_{i/o}$ cRNAs (Fig. 3*B*). The observed changes in $^{35}$S labelling were also paralleled by densitometric changes in the bands detected by Western blot analysis (Fig. 3*B*). Since the peak $I_{K,ACh}$ amplitudes for $G\alpha_o$-coupled m2 receptors were ~2 times higher compared to $G\alpha_i$-coupled m2 receptors under equivalent expression conditions (cf. Fig. 2*B*), the ~2-fold difference in $G\alpha_{oB(C351G)}$ *versus* $G\alpha_{i2(C352G)}$ or $G\alpha_{i3(C351G)}$ protein expression could potentially account for the differences in m2 receptor-GIRK channel coupling. $G\alpha_{oA(C351G)}$-elevated protein levels, however, were similar to $G\alpha_{i2(C352G)}$ and $G\alpha_{i3(C351G)}$ levels (Fig. 3*B*), and resolving small expression changes was clearly limited by the biochemical approach. Thus despite equivalent cRNA injections (5 ng cRNA/oocyte each), differences in $G\alpha_{i/o}$ biosynthesis and/or degradation may result in different steady-state $G\alpha_{i/o}$ protein levels that account for the distinct gating properties of $G\alpha_o$- *versus* $G\alpha_i$-coupled GIRK currents.

### The GIRK activation time course is dependent on free $G\beta\gamma$ levels

A sigmoidal time course for GIRK activation, as observed with $G\alpha_o$ expression (Fig. 2), is well documented in cardiomyocytes and neurons and indicative of a multi-step process in channel opening (Inomata *et al.* 1989; Sodickson & Bean, 1996). Tetrameric GIRK channels can bind up to four $G\beta\gamma$ dimers, and functional studies indicate at least two $G\beta\gamma$ dimers are necessary for channel opening (Nemec *et al.* 1999; Corey & Clapham, 2001). We questioned whether the sigmoidal GIRK activation time course via $G\alpha_o$-coupled receptors was a consequence of a markedly reduced free $G\beta\gamma$ concentration as indicated by the low $I_{K,basal}$ level. As illustrated in Fig. 4*A*, conditions favouring high free $G\beta\gamma$ concentrations (high $I_{K,basal}$) would yield a single exponential time course for receptor activation, where the binding of a single $G\beta\gamma$ dimer leads to channel opening. At low free $G\beta\gamma$ concentrations (i.e. low $I_{K,basal}$), GIRK channels would instead be occupied by fewer $G\beta\gamma$ dimers (less than 3 $G\beta\gamma$) and require multiple $G\beta\gamma$ binding events during receptor activation (2–4 $G\beta\gamma$). According to this hypothesis, reducing $G\alpha_o$ expression levels should increase $I_{K,basal}$ and promote a single exponential time course for $I_{K,ACh}$ activation.

To test this, we compared the activation time course of $I_{K,ACh}$ at two different levels of $G\alpha_{oB(C351G)}$ expression (Fig. 4). As expected, lower expression of $G\alpha_{oB(C351G)}$ (1 ng $G\alpha_{oB(C351G)}$ cRNA/oocyte) produced smaller $I_{K,ACh}$ amplitudes compared to high $G\alpha_{oB(C351G)}$ expression, and had significantly higher receptor-independent basal GIRK activity (Fig. 4*C* and *D*). The activation time course for $I_{K,ACh}$ was clearly affected by the level of $G\alpha_{oB(C351G)}$ expression and was consistent with the gating scheme shown in Fig. 4*A*. Low $G\alpha_{oB(C351G)}$ expression yielded GIRK currents whose activation time course was well described by a single exponential function. In contrast, high $G\alpha_{oB(C351G)}$ expression yielded GIRK currents whose activation time course had a significant delay and were best described by a 3rd order exponential function, suggesting the binding of three $G\beta\gamma$ subunits in receptor-dependent GIRK activation (see Fig. 4*A*). The $\tau_{act}$ was smaller for high

receptor activation. *B*, left panel: ACh-evoked GIRK currents from oocytes injected with either 1 or 5 ng $G\alpha_{oB(C351G)}$ cRNA. Right panel: the activation phase for the 1 $\mu$M ACh-evoked GIRK currents are displayed at higher temporal resolution. Red lines represent non-linear fits to the data. A single exponential function (G1) best described the $I_{K,ACh}$ time course with low $G\alpha_{oB(C351G)}$ expression (1 ng RNA/oocyte), having a time constant of 8.1 s. A third-order exponential function (G3) best described the activation time course at high $G\alpha_{oB(C351G)}$ expression (5 ng RNA/oocyte), having a time constant of 4.4 s. *C*, ACh dose–response curves for m2 receptor-activated GIRK currents from control oocytes (○) and oocytes expressing $G\alpha_{oB(C351G)}$ at two different levels (■ 1 ng and ▲ 5 ng cRNA/oocyte). *D*, effects of $G\alpha_{oB(C351G)}$ expression levels on receptor-independent GIRK channel activity ($I_{K,basal}$). The open bar is from control oocyte responses, and black bars are from oocytes injected with varying amount of $G\alpha_{oB(C351G)}$ cRNA and PTX-S1 cRNA (1 ng/oocyte). Data represent the means + S.E.M. from 4 batches of oocytes with the number of oocytes indicated.

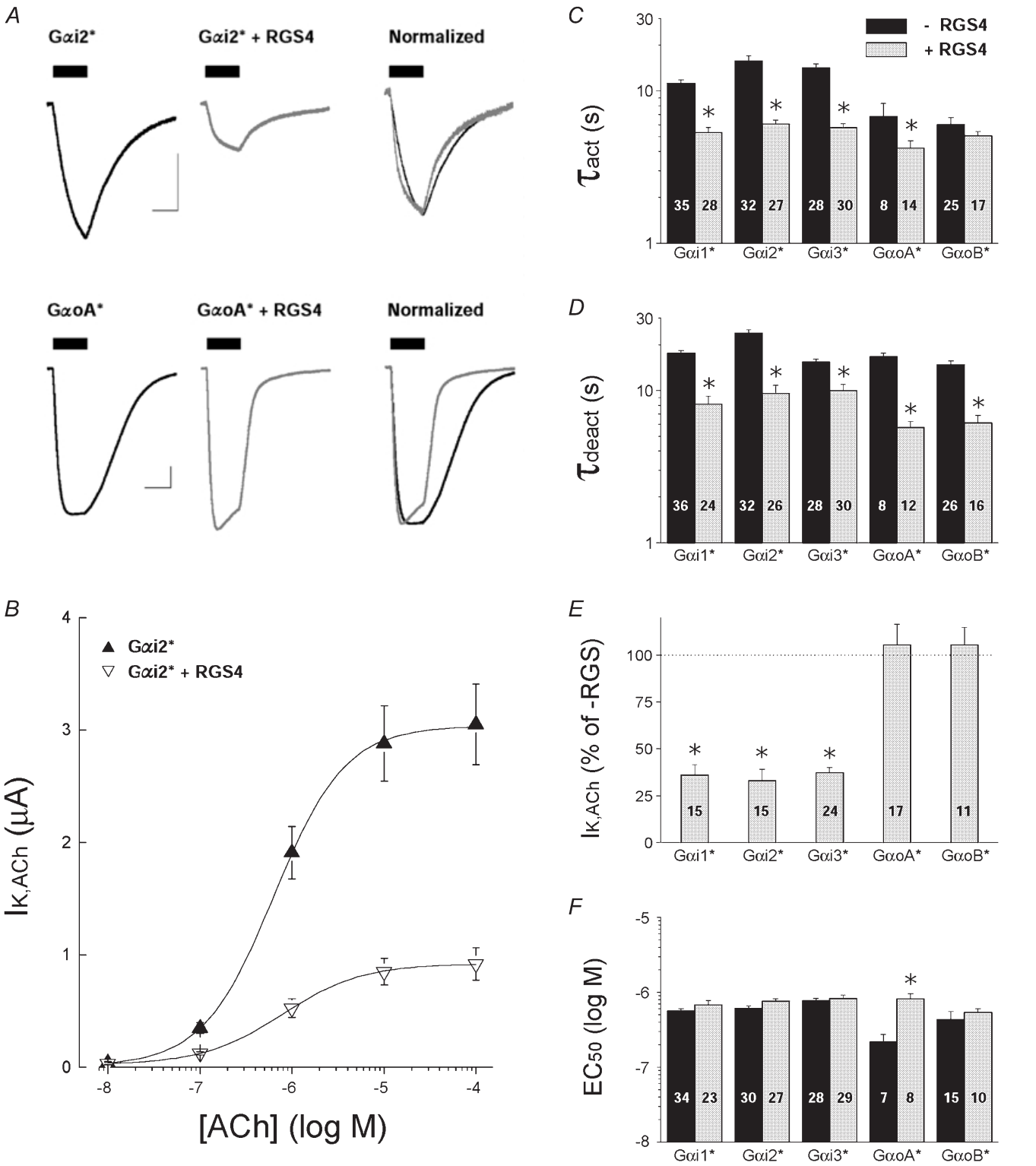


**Figure 5. Effects of RGS4 on GIRK currents coupled to specific PTX-insensitive G$\alpha_{i/o}$ subunits**

All data are from oocytes injected with 5 ng G$\alpha$* cRNA/oocyte, with or without 10 ng RGS4 cRNA/oocyte. Endogenous PTX-sensitive G$\alpha_{i/o}$ subunits were inactivated by either PTX injection or PTX-S1 expression as described in Methods. Data are means and S.E.M.; * $P < 0.05$. *A*, representative ACh-evoked GIRK currents from oocytes expressing either G$\alpha_{i2(C352G)}$ (upper traces) or G$\alpha_{oA(C351G)}$ (lower traces) with and without RGS4 coexpression. Scale bars indicate 1 $\mu$A and 10 s. *B*, ACh dose–response relations for m2 receptor-coupled GIRK currents from oocytes expressing G$\alpha_{i2(C352G)}$ in the absence (▲) or presence of RGS4 (▽). *C*, $I_{K,ACh}$ activation time constants ($\tau_{act}$) from oocytes expressing PTX-insensitive G$\alpha_{i/o}$ subunits alone (black bars) or with co-expressed RGS4 (grey bars). Time constants were derived from a single exponential fit to the rising

$G\alpha_{oB(C351G)}$ expression *versus* low $G\alpha_{oB(C351G)}$ expression, and single exponential fits to the rising phase of the sigmoidal time course underestimate the activation rate constant ($1/\tau_{act}$) under these conditions. Comparisons of $\tau_{deact}$ and $EC_{50}$ values from ACh dose–response curves indicated the these properties were not significantly affected by these levels of $G\alpha_{oB(C351G)}$ expression (data not shown).

### RGS4 reduces GIRK currents at low $G\alpha_{i/o}$ coupling levels

We next evaluated the effects of RGS4 at saturating expression levels (10 ng RGS4 cRNA/oocyte; Doupnik *et al.* 1997; Keren-Raifman *et al.* 2001) on both $G\alpha_o$- and $G\alpha_i$-coupled m2 receptors as described in Fig. 2. As shown in Fig. 5, RGS4 accelerated the receptor-dependent GIRK activation and deactivation kinetics for each $G\alpha_{i/o}$ isoform, consistent with the non-selective GTPase activating properties of RGS4 on $G\alpha_{i/o}$ subunits *in vitro* (Berman *et al.* 1996; Watson *et al.* 1996). Interestingly, however, RGS4 suppressed 60–70 % of the $I_{K,ACh}$ amplitude for $G\alpha_i$-coupled m2 receptors, yet had no effect on the peak $I_{K,ACh}$ amplitude of $G\alpha_o$-coupled receptors. RGS4 did not significantly affect the $EC_{50}$ for channel activation via $G\alpha_i$-coupled receptors, but did cause a small shift the $EC_{50}$ value for $G\alpha_{oA(C351G)}$-coupled GIRK currents towards a higher ACh concentration, which more closely corresponded to the $EC_{50}$ values of $G\alpha_i$-coupled GIRK currents (Fig. 5*F*). Kinetic analysis indicated the RGS4-mediated reduction in $G\alpha_i$-coupled $I_{K,ACh}$ (Fig. 5*E*) was fully explained by the RGS4-accelerated GIRK deactivation rate (see Table 2 and Discussion).

To determine whether the higher degree of $G\alpha_o$ *versus* $G\alpha_i$ coupling (cf. Fig. 2) could account for the RGS4-dependent effects on steady-state GIRK currents, we examined the effects of RGS4 at a lower level of $G\alpha_{oA}$ expression (0.5 ng cRNA/oocyte). At low $G\alpha_{oA}$ expression levels, RGS4 significantly reduced ~90 % of both $I_{K,ACh}$ ($G\alpha_{oA}$ alone, $0.76 \pm 0.11$ $\mu$A, $n = 17$; $G\alpha_{oA}$ + RGS4, $0.07 \pm 0.03$ $\mu$A, $n = 9$; $P < 0.05$) and $I_{K,basal}$ ($G\alpha_{oA}$ alone, $2.34 \pm 0.18$ $\mu$A, $n = 19$; $G\alpha_{oA}$ + RGS4, $0.25 \pm 0.07$ $\mu$A, $n = 14$; $P < 0.05$). Thus the effect of RGS4 on steady-state GIRK current amplitudes is dependent on the level of $G\alpha_{i/o}$ expression and GPCR precoupling. At high levels of m2 receptor-$G\alpha_o$ coupling (i.e. Fig. 5), RGS4 accelerates GIRK activation and deactivation without significantly reducing steady-state GIRK current amplitudes and resembles the effects of RGS4 with endogenous $xG\alpha_{i/o}$ coupling (Doupnik *et al.* 1997).

### RGS7 selectively accelerates $G\alpha_o$-coupled GIRK currents

RGS7 belongs to a distinct subfamily of RGS proteins that contain a G$\gamma$-like (GGL) domain that specifically binds G$\beta$5 subunits (Snow *et al.* 1998; Sondek & Siderovski, 2001). RGS7 has relatively weak effects on GIRK current kinetics when expressed without G$\beta$5 in *Xenopus* oocytes (Saitoh *et al.* 1999), but is significantly enhanced by G$\beta$5 co-expression (Kovoor *et al.* 2000; Keren-Raifman *et al.* 2001). We examined whether RGS7 (10 ng cRNA/oocyte), with or without co-expressed G$\beta$5 subunits, differentially affected $G\alpha_o$- *versus* $G\alpha_i$-coupled GIRK currents. In the absence of coexpressed G$\beta$5, RGS7 preferentially accelerated $G\alpha_o$-coupled GIRK currents having little effect on $G\alpha_i$-coupled GIRK kinetics (Fig. 6), which is consistent with other studies indicating RGS7 selectively interacts with $G\alpha_o$ subunits (Posner *et al.* 1999; Lan *et al.* 2000; Rose *et al.* 2000). Interestingly, RGS7 acceleration of $G\alpha_o$-coupled $I_{K,ACh}$ was greater than that caused by RGS4 (cf. Fig. 5*C* and *D*) and was evident for both the $I_{K,ACh}$ activation and deactivation time course as well as the desensitization rate. As observed with RGS4, RGS7 did not cause a significant reduction in the maximal $G\alpha_o$-coupled GIRK current despite accelerating the GIRK channel gating kinetics (Fig. 6*E*), but did cause a small shift in the ACh dose–response curve (Fig. 6*B* and *F*). Yet in contrast to RGS4, RGS7 did not reduce steady-state GIRK currents when $G\alpha_{oA}$ expression was markedly reduced (0.5 ng cRNA/oocyte): $I_{K,basal}$ ($G\alpha_{oA}$ alone, $2.34 \pm 0.18$ $\mu$A, $n = 19$; $G\alpha_{oA}$ + RGS7, $2.18 \pm 0.20$ $\mu$A, $n = 18$) and $I_{K,ACh}$ ($G\alpha_{oA}$ alone, $0.76 \pm 0.11$ $\mu$A, $n = 17$; $G\alpha_{oA}$ + RGS7, $1.25 \pm 0.21$ $\mu$A, $n = 17$).

### RGS7-G$\beta$5 disrupts $G\alpha_o$-coupled GIRK currents

G$\beta$5 binds with high affinity to the GGL domain of RGS7, enhancing the GAP activity and protein stability of RGS7 (Levay *et al.* 1999; Kovoor *et al.* 2000; Keren-Raifman *et al.* 2001). We examined the effects of G$\beta$5 expression on the RGS7- mediated regulation of both $G\alpha_o$- and $G\alpha_i$-coupled GIRK currents, with comparisons made using G$\beta$1 as a negative control which does not bind to RGS7 (Levay *et al.* 1999; Kovoor *et al.* 2000). As shown in Fig. 7, co-expression of G$\beta$5 with RGS7 caused a significant

phase of $I_{K,ACh}$ elicited by 1 $\mu$M ACh. *D*, deactivation time constants ($\tau_{deact}$) derived from ACh-elicited GIRK currents recorded from oocytes expressing PTX-insensitive $G\alpha_{i/o}$ subunits alone (black bars) or with co-expressed RGS4 (grey bars). Time constants were derived from a single exponential fit to the decay of $I_{K,ACh}$ after rapid washout of 1 $\mu$M ACh. *E*, effects of RGS4 on maximal $I_{K,ACh}$ responses elicited by m2 receptors coupled to PTX-insensitive $G\alpha_{i/o}$ subunits. $I_{K,ACh}$ amplitudes (10 $\mu$M ACh) from RGS4-expressing oocytes are expressed as a percentage of the mean $I_{K,ACh}$ amplitude from oocytes expressing the PTX-insensitive $G\alpha_{i/o}$ subunit alone (RGS-). *F*, effects of RGS4 on the $EC_{50}$ for ACh activation of GIRK currents coupled to m2 receptors and PTX-insensitive $G\alpha_{i/o}$ subunits. Black bars are without RGS4 expression (−RGS4), grey bars are with RGS4 co-expression (+RGS4).

Journal of Physiology

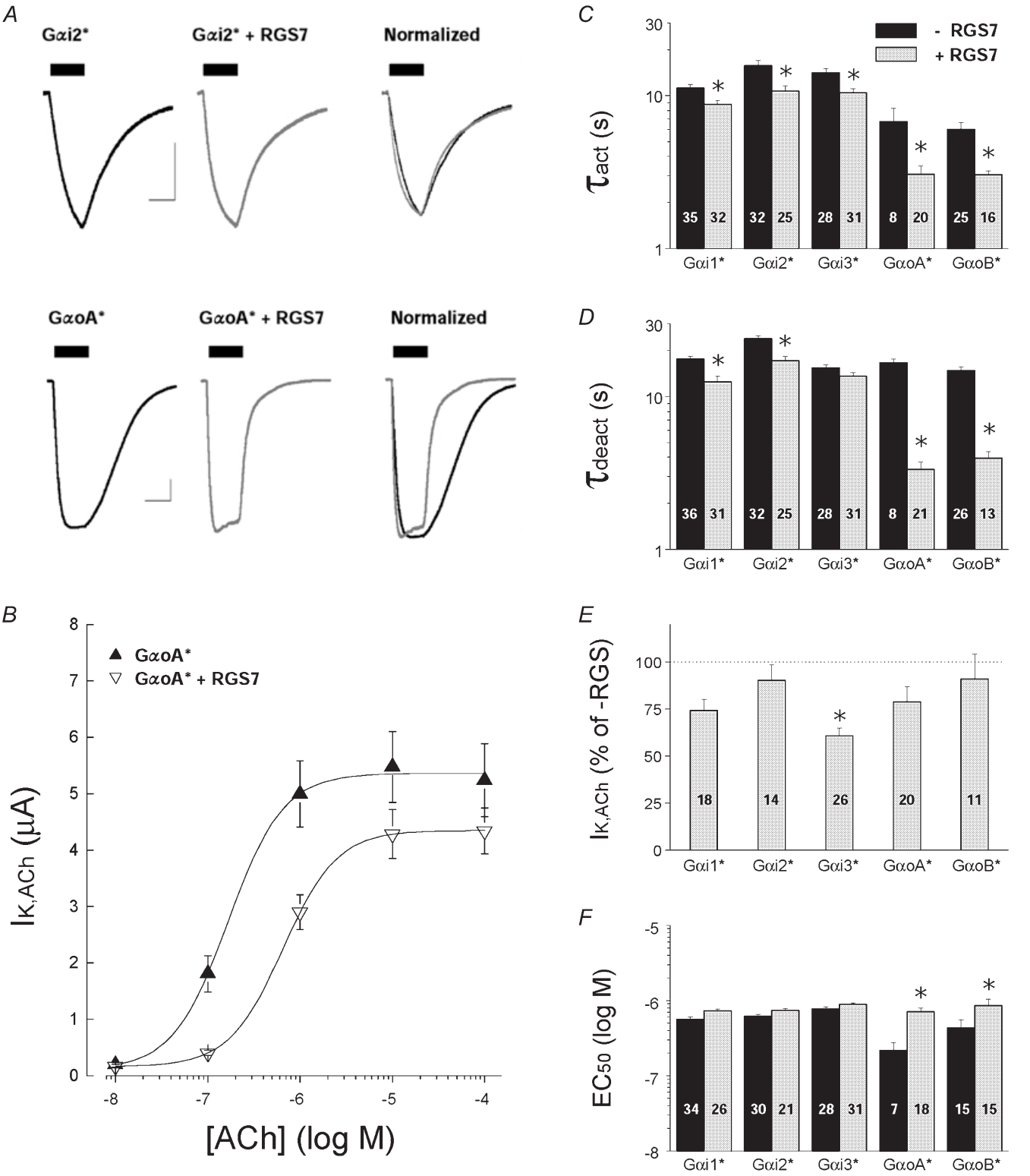


**Figure 6. Effects of RGS7 on GIRK currents coupled to specific PTX-insensitive G$\alpha_{i/o}$ subunits**

All data are from oocytes injected with 5 ng G$\alpha$* cRNA/oocyte, with or without 10 ng RGS7 cRNA/oocyte. Endogenous PTX-sensitive G$\alpha_{i/o}$ subunits were inactivated by either PTX injection or PTX-S1 expression as described in Methods. Data are means and S.E.M.; * $P < 0.05$. *A*, representative ACh-evoked GIRK currents from oocytes expressing either G$\alpha_{i2(C352G)}$ (upper traces) or G$\alpha_{oA(C351G)}$ (lower traces) with and without RGS7 coexpression. Scale bars indicate 1 $\mu$A and 10 s. *B*, ACh dose–response relations for m2 receptor-coupled GIRK currents from oocytes expressing G$\alpha_{i2(C352G)}$ in the absence (▲) or presence of RGS7 (▽). *C*, $I_{K,ACh}$ activation time constants ($\tau_{act}$) from oocytes expressing PTX-insensitive G$\alpha_{i/o}$ subunits alone (black bars) or with co-expressed RGS7 (grey bars). Time constants are from GIRK currents evoked by 1 $\mu$M ACh.

reduction (70–80 %) in $G\alpha_o$-coupled GIRK current amplitudes, yet had no effect on $G\alpha_i$-coupled currents. The lack of effect of $G\beta5$ on $G\alpha_i$-coupled GIRK currents indicates the level of $G\beta5$ (or $G\beta5\gamma$ formation) does not cause a direct inhibition of GIRK currents as observed in transfected HEK-293 cells (Lei *et al.* 2000). In addition to reducing $G\alpha_o$-coupled GIRK currents, $G\beta5$ enhanced the RGS7-accelerated GIRK kinetics consistent with RGS7-$G\beta5$ complexes having greater GAP activity compared to RGS7 alone (Kovoor *et al.* 2000; Keren-Raifman *et al.* 2001). Thus the formation of RGS7–$G\beta5$ complexes apparently disrupts $G\alpha_o$ coupling (either to m2 receptors and/or GIRK channels) and is supported by the effects of $G\beta5$ on RGS7–$G\alpha_o$ interactions *in vitro* (Levay *et al.* 1999).

## DISCUSSION

The goal of this study was to determine whether functional differences exist in the GPCR-dependent gating properties of GIRK channels coupled to specific $G\alpha_{i/o}$ subunits and RGS proteins. Our findings reveal that m2 receptors coupled to $G\alpha_i$ and $G\alpha_o$ subunits are differentially regulated by RGS4 and RGS7. A significant finding of our study is the identification of G protein coupling levels as a critical determinant in mediating the anomalous kinetic effects of RGS proteins on GIRK channel gating (Doupnik *et al.* 1997; Saitoh *et al.* 1997; Zerangue & Jan, 1998; Kovoor & Lester, 2002). Incremental increases in $G\alpha_o\beta\gamma$ coupling by increased $G\alpha_o$ expression revealed a transition in the RGS4-accelerated GIRK currents from 'expected' steady-state properties, characterized by a large reduction in maximal GIRK current amplitude, to 'anomalous' gating kinetics which displayed accelerated activation and deactivation kinetics with no effect on steady-state GIRK amplitude. We propose that this transition in steady-state GIRK channel kinetics is a functional indicator of the formation of a GPCR–G protein–GIRK channel signalling complex (Huang *et al.* 1995; Slesinger *et al.* 1995) that is precipitated at a critical level of $G\alpha_{i/o}$ expression and revealed by the modulatory actions of co-expressed RGS proteins.

### RGS proteins reveal GPCR–G protein–GIRK coupling levels via steady-state gating properties

RGS proteins were originally identified as 'negative regulators' of G protein signalling causing reduced GPCR signalling in yeast, fungi, nematodes and mammals (Dohlman *et al.* 1995, 1996; Druey *et al.* 1996; Koelle & Horvitz, 1996; Yu *et al.* 1996). These findings were readily explained by RGS proteins behaving as GTPase-activating proteins and accelerating the termination of G protein signalling (Berman *et al.* 1996; Chen *et al.* 1996; Hunt *et al.* 1996; Watson *et al.* 1996). Initial studies of the effects of RGS proteins on GPCR-evoked GIRK currents revealed the anticipated acceleration in current deactivation, which was well explained by the RGS-accelerated GTPase activity of $G\alpha_{i/o}$ subunits causing a more rapid sequesteration of channel-activating $G\beta\gamma$ dimers (Doupnik *et al.* 1997; Saitoh *et al.* 1997). Unexpectedly, however, the accelerated deactivation was also accompanied with an accelerated activation phase in the absence of reduced current amplitude.

We analysed the temporal and steady-state GIRK current kinetics for the various conditions tested in this study using a simplified two-state gating scheme (Doupnik *et al.* 1997):

$$\text{Closed} \underset{k_{\text{close}}}{\overset{k_{\text{open[G]}}}{\rightleftharpoons}} \text{Open}$$

where the forward rate constant for GIRK channel opening ($k_{open}$) is dependent on the rate of $G\beta\gamma$ production during GPCR activation (Breitwieser & Szabo, 1988; Yamada *et al.* 1998), and the closing rate constant ($k_{close}$) is dependent on $G\beta\gamma$ clearance, which is rate-limited by the GTP hydrolysis rate of $G\alpha$ subunits. Accordingly, the time constant for GIRK channel deactivation ($\tau_{deact}$) is equal to $k_{close}^{-1}$, and the time constant for GIRK activation ($\tau_{act}$) is equal to $(k_{open} + k_{close})^{-1}$ (Doupnik *et al.* 1997). Using these relations and an empirically derived $k_{open}$ value of 0.03 $s^{-1}$ (held constant to simulate a saturating agonist concentration), the experimentally derived $\tau_{deact}$ values were used to calculate 'expected' values of $\tau_{act}$ and steady-state GIRK current amplitudes ($k_{open}/[k_{open} + k_{close}]$) in the absence and presence of RGS expression according to the kinetic model. The 'expected' values were then compared to the experimentally 'observed' values (Table 2).

As seen in Table 2, the 'observed' effects of RGS4 on $\tau_{act}$ and steady-state amplitude for $G\alpha_i$-coupled GIRK currents closely correlate with the 'expected' consequences of the RGS4-accelerated deactivation rate, but not so for the $G\alpha_o$-coupled GIRK currents. Similarly, a correlation was seen for the effects of $G\beta5$ on RGS7-accelerated GIRK

*D,* deactivation time constants ($\tau_{deact}$) from ACh-elicited GIRK currents recorded from oocytes expressing PTX-insensitive $G\alpha_{i/o}$ subunits alone (black bars) or with co-expressed RGS7 (grey bars). Time constants were derived after rapid washout of 1 $\mu$M ACh. *E,* effects of RGS7 on maximal $I_{K,ACh}$ responses elicited by m2 receptors coupled to PTX-insensitive $G\alpha_{i/o}$ subunits. $I_{K,ACh}$ amplitudes (10 $\mu$M ACh) from RGS4-expressing oocytes as a percentage of the mean $I_{K,ACh}$ amplitude from oocytes expressing the PTX-insensitive $G\alpha_{i/o}$ subunit alone (no RGS7). *F,* effects of RGS7 on the $EC_{50}$ for ACh activation of GIRK currents coupled to m2 receptors and PTX-insensitive $G\alpha_{i/o}$ subunits. Black bars are without RGS7 expression, grey bars are with RGS7 co-expression.

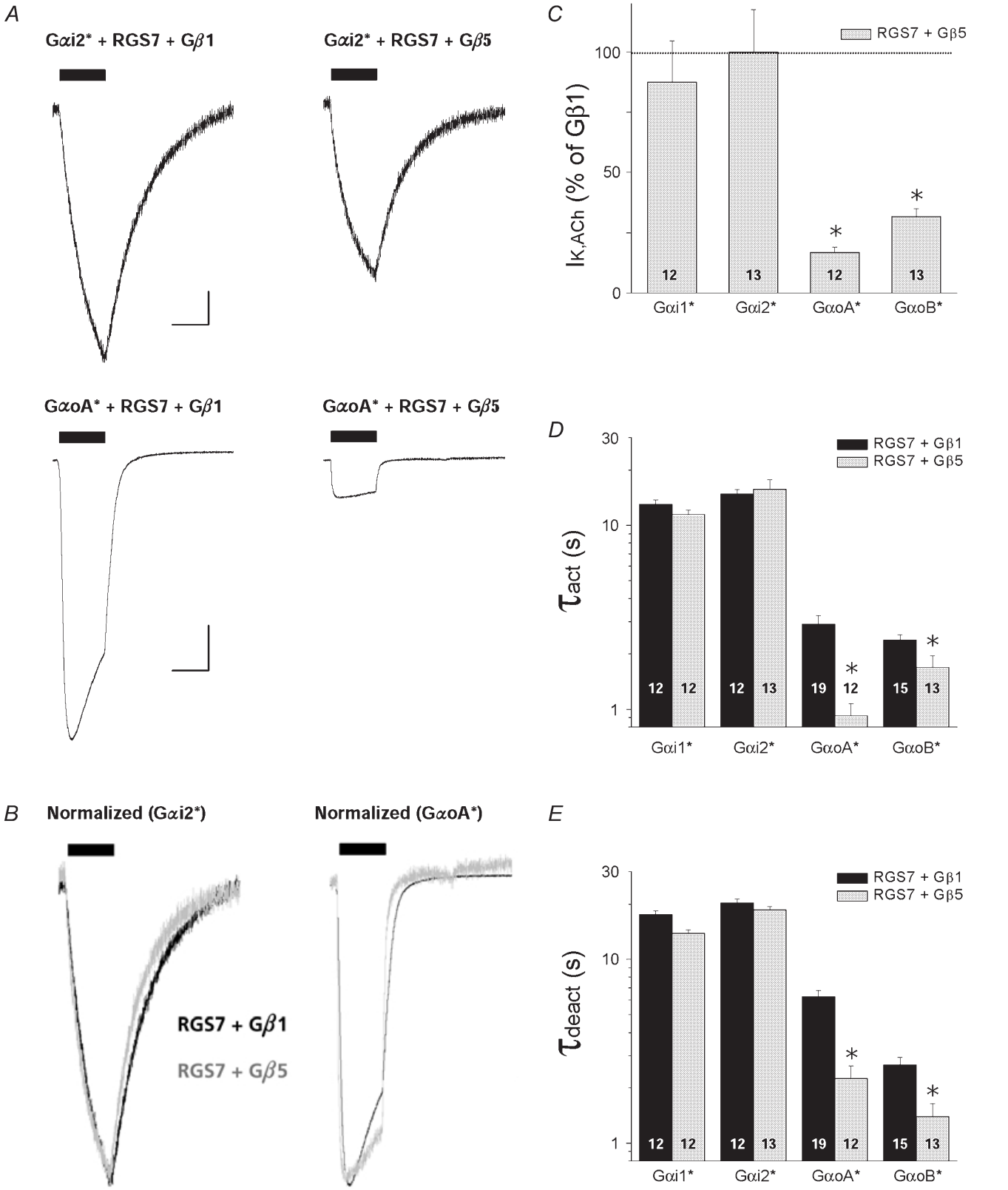


**Figure 7. Effects of Gβ5 on RGS7-accelerated GIRK currents coupled to specific PTX-insensitive $G\alpha_{i/o}$ subunits**

All data are from oocytes injected with 5 ng Gα* cRNA/oocyte and 10 ng RGS7 cRNA/oocyte, with either 5 ng Gβ5 cRNA/oocyte or 5 ng Gβ1 cRNA/oocyte as a negative control. Oocytes also received Kir3.1 and Kir3.2a cRNA (0.5 ng/oocyte each), and m2 receptor cRNA (0.5 ng/oocyte), and endogenous PTX-sensitive $G\alpha_{i/o}$ subunits were inactivated by PTX-S1 expression (1.0 ng/oocyte). Data are means + S.E.M.; * $P < 0.05$.

**Table 2: 'Expected' versus 'Observed' gating parameters for RGS-accelerated GIRK currents**

| Expressed proteins | Observed $\tau_{deact}$ (s) | Expected mean $\tau_{act}$ (s) | Observed $\tau_{act}$ (s) | Expected amplitude (% of control) | Observed amplitude (% of control) |
|---|---|---|---|---|---|
| $G\alpha_{i1}$* | 17.6 ± 4.6 | 11.5 | 11.2 ± 3.8 | — | — |
| $G\alpha_{i1}$* + RGS4 | 8.1 ± 5.0 | 6.5 | 5.3 ± 2.2 | 56 ± 28 | 36 ± 5 |
| $G\alpha_{I1}$* + RGS7 | 12.5 ± 6.1 | 9.1 | 8.8 ± 2.9 | 79 ± 25 | 74 ± 6 |
| $G\alpha_{i1}$* + RGS7 + G$\beta$1 | 17.5 ± 2.9 | 11.5 | 13.0 ± 2.6 | — | — |
| $G\alpha_{i1}$* + RGS7 + G$\beta$5 | 13.9 ± 2.1 | 9.8 | 11.4 ± 2.5 | 85 ± 9 | 88 ± 17 |
| $G\alpha_{i2}$* | 23.8 ± 7.1 | 13.9 | 15.7 ± 7.1 | — | — |
| $G\alpha_{i2}$* + RGS4 | 9.6 ± 6.3 | 7.5 | 6.1 ± 2.1 | 54 ± 23 | 33 ± 6 |
| $G\alpha_{i2}$* + RGS7 | 17.1 ± 6.4 | 11.3 | 10.8 ± 4.3 | 81 ± 18 | 90 ± 8 |
| $G\alpha_{i2}$* + RGS7 + G$\beta$1 | 20.3 ± 3.6 | 12.6 | 14.8 ± 2.9 | — | — |
| $G\alpha_{i2}$* + RGS7 + G$\beta$5 | 18.6 ± 2.9 | 11.9 | 15.7 ± 7.5 | 95 ± 9 | 100 ± 18 |
| $G\alpha_{i3}$* | 15.4 ± 3.4 | 10.5 | 14.1 ± 5.2 | — | — |
| $G\alpha_{i3}$* + RGS4 | 10.0 ± 5.3 | 7.7 | 5.7 ± 2.0 | 73 ± 27 | 37 ± 3 |
| $G\alpha_{i3}$* + RGS7 | 13.5 ± 4.4 | 9.6 | 10.5 ± 3.6 | 91 ± 20 | 61 ± 4 |
| $G\alpha_{oA}$* | 16.7 ± 2.8 | 11.1 | 6.8 ± 4.1 | — | — |
| $G\alpha_{oA}$* + RGS4 | 5.7 ± 1.9 | 4.9 | 4.2 ± 1.9 | 44 ± 12 | 105 ± 11† |
| $G\alpha_{oA}$* + RGS7 | 3.3 ± 1.7 | 3.0 | 3.1 ± 1.8 | 27 ± 12 | 79 ± 8† |
| $G\alpha_{oA}$* + RGS7 + G$\beta$1 | 6.3 ± 2.2 | 5.3 | 2.9 ± 1.5 | — | — |
| $G\alpha_{oA}$* + RGS7 + G$\beta$5 | 2.2 ± 1.3 | 2.0 | 0.9 ± 0.5 | 39 ± 21 | 17 ± 2 |
| $G\alpha_{oB}$* | 14.8 ± 4.9 | 10.3 | 6.0 ± 3.4 | — | — |
| $G\alpha_{oB}$* + RGS4 | 6.1 ± 2.9 | 5.2 | 5.0 ± 1.4 | 50 ± 19 | 105 ± 9† |
| $G\alpha_{oB}$* + RGS7 | 4.0 ± 1.5 | 3.6 | 3.1 ± 0.7 | 35 ± 11 | 91 ± 13† |
| $G\alpha_{oB}$* + RGS7 + G$\beta$1 | 2.7 ± 1.0 | 2.5 | 2.4 ± 0.7 | — | — |
| $G\alpha_{oB}$* + RGS7 + G$\beta$5 | 1.4 ± 0.9 | 1.3 | 1.7 ± 1.0 | 54 ± 32 | 32 ± 3 |

† denotes deviation from expected steady-state GIRK current amplitude.

currents activated by $G\alpha_o$-coupled receptors. Thus during reduced levels of G protein coupling, GIRK channels behave according to standard kinetic concepts in response to RGS modulation and are consistent with the collision coupling model of G protein activation (Shea & Linderman, 1997; Shea *et al.* 2000). In contrast, RGS4 and RGS7 modulate $G\alpha_o$-coupled GIRK currents in a manner similar to previous descriptions of the anomalous kinetic effects of RGS proteins on GIRK channel gating which do not correlate with the kinetic model (Table 2) (Doupnik *et al.* 1997; Saitoh *et al.* 1997). We propose that these expression conditions promote the formation of a precoupled m2 receptor–$G\alpha_o\beta\gamma$–GIRK channel complex (Huang *et al.* 1995; Slesinger *et al.* 1995), having altered activation properties that are revealed by the modulatory effects of RGS proteins and effectively preserve maximal GIRK current amplitudes (see Fig. 8).

## GIRK activation kinetics revealed at low levels of basal activity

GIRK channels are composed of four Kir3.0 subunits with each subunit capable of binding a single $G\beta\gamma$ dimer, thus a maximum of four $G\beta\gamma$ dimers can bind to a single GIRK channel (Corey & Clapham, 2001). Several studies indicate GIRK channel activation is a multi-step process and may

*A*, representative ACh-evoked GIRK currents from oocytes expressing RGS7 and $G\alpha_{i2(C352G)}$ with either G$\beta$1 or G$\beta$5 (upper traces), or $G\alpha_{oA(C351G)}$ with either G$\beta$1 or G$\beta$5 (lower traces). Scale bars indicate 1 $\mu$A and 10 s. *B*, GIRK currents from *A*, normalized to peak amplitude and superimposed to highlight their temporal features (black traces, RGS7+G$\beta$1; grey traces, RGS7+G$\beta$5). *C*, G$\beta$5 selectively suppresses RGS7/ Gαo-coupled GIRK currents. $I_{K,ACh}$ amplitudes are expressed as a percentage of the mean $I_{K,ACh}$ amplitude from oocytes expressing the negative control G$\beta$1. *D*, GIRK activation time constants ($\tau_{act}$) derived from oocytes expressing different PTX-insensitive $G\alpha_{i/o}$ subunits with either RGS7 + G$\beta$1 (black bars) or RGS7 + G$\beta$5 (grey bars). Time constants were derived from a single exponential fit to the rising phase of $I_{K,ACh}$ elicited by 1 $\mu$M ACh. *E*, deactivation time constants ($\tau_{deact}$) derived from ACh-elicited GIRK currents as in *D*. Time constants were derived from a single exponential fit to the decay of $I_{K,ACh}$ after rapid washout of 1 $\mu$M ACh.

represent the binding of multiple G$\beta\gamma$ dimers leading to channel opening (Hosoya *et al.* 1996; Sodickson & Bean, 1996; Nemec *et al.* 1999). Assuming four bound G$\beta\gamma$ dimers promote the channel open state, receptor-independent basal GIRK activity represents channels transiently occupied by four G$\beta\gamma$ dimers, excluding the potential influence of phosphatidylinositol-4,5-bisphosphate ($PIP_2$), arachidonic acid, and intracellular $Na^+$, $Mg^{+2}$ and polyamines (Dascal, 1997; Yamada *et al.* 1998). $I_{K,basal}$ activity is directly related to the concentration of free G$\beta\gamma$ in the cell membrane based on the effectiveness of G$\beta\gamma$ scavengers to lower $I_{K,basal}$ amplitudes (Lim *et al.* 1995; Vivaudou *et al.* 1997; Jeong & Ikeda, 1999; Fernandez-Fernandez *et al.* 2001). According to the GIRK channel gating scheme shown in Fig. 4*A*, basal GIRK activity reflects channels transiently occupied by three to four G$\beta\gamma$ dimers where random association of a single free G$\beta\gamma$ subunit causes channel opening. Receptor activation of GIRK channels with high free G$\beta\gamma$ concentrations predict a single G$\beta\gamma$ binding event is necessary to activate the channels and $I_{K,ACh}$ will thus follow a single exponential time course. Conversely, receptor activation with low concentrations of free G$\beta\gamma$ predict multiple binding events are necessary for channel opening, producing a sigmoidal $I_{K,ACh}$ time course analogous to the sequential movement of multiple gates during the activation of voltage-gated ion channels (Hodgkin & Huxley, 1952). The observed time course for receptor-

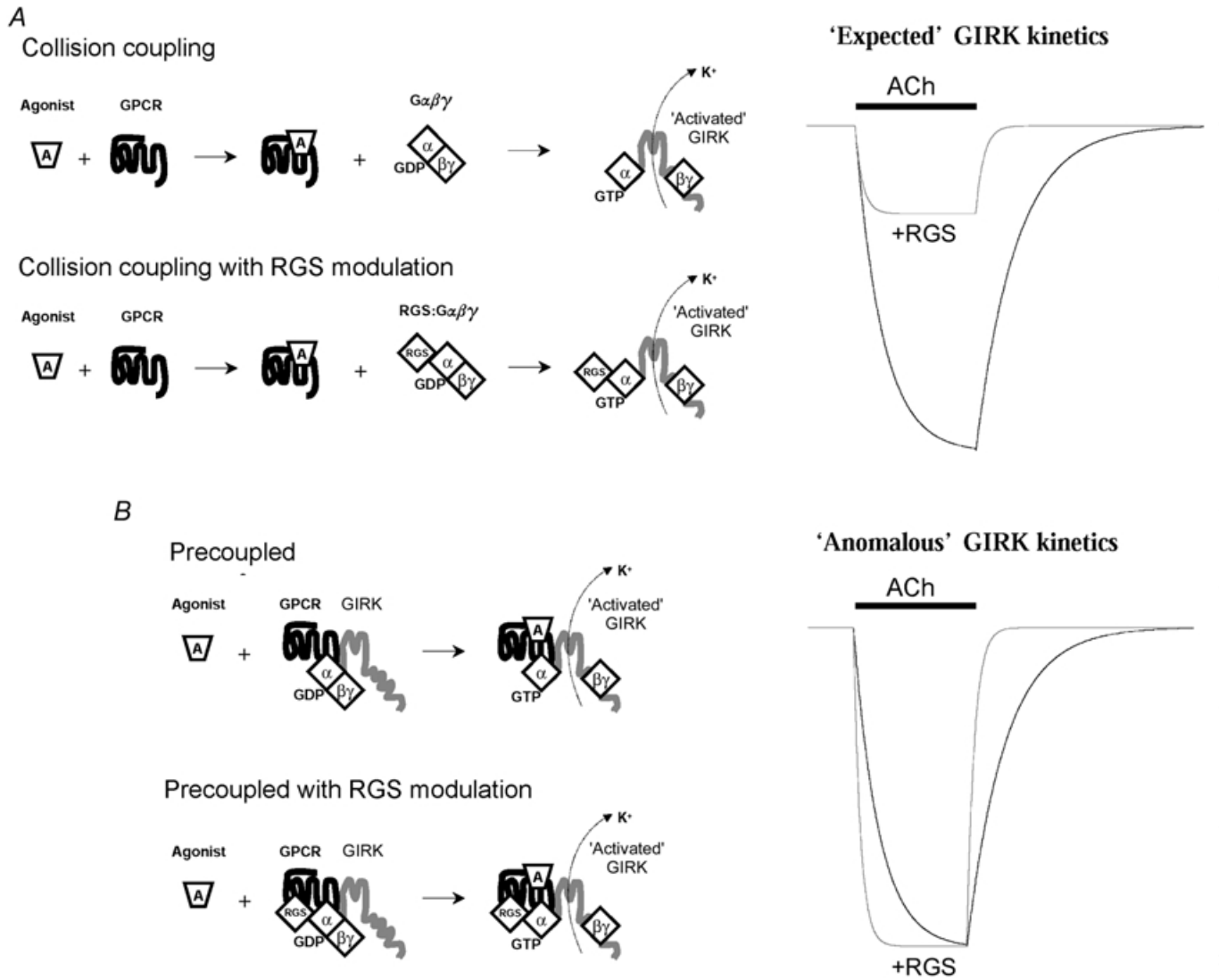


**Figure 8. RGS modulation of GPCR → GIRK signal transduction at varying levels of G protein coupling**

*A*, collision coupling model (low G$\alpha$ expression) and *B* precoupled model (high G$\alpha$ expression). The precoupled model assumes a GPCR–G protein–RGS–GIRK channel complex displaying 'anomalous' kinetic behaviour that was characteristic of oocytes expressing $G\alpha_o$ subunits with either RGS4 or RGS7, together with co-expressed m2 receptors and GIRK channel Kir3.1/3.2a subunits.

dependent GIRK activation at the different levels of basal activity produced by high and low levels of $G\alpha_o$ expression are in agreement with this and similar GIRK gating schemes (Destexhe & Sejnowski, 1995; Hosoya *et al.* 1996; Ivanova-Nikolova *et al.* 1998; Yamada *et al.* 1998). Different levels of GIRK–$G\beta\gamma$ occupancy may also influence the voltage-dependent relaxation phenomena associated with RGS4 expression, which is only observed at low agonist concentrations (Inanobe *et al.* 2001). Although we deliberately express low levels of m2 receptors to slow GIRK activation rates (Herlitze *et al.* 1999), it should be emphasized that the GIRK activation and deactivation kinetics measured in the oocyte expression system, even with RGS expression, are consistently slower than native mammalian cells and may be limited by solution exchange rates and/or other intrinsic oocyte factors.

Interestingly, overexpression of a PTX-insensitive and RGS-resistant $G\alpha_o$ mutant ($G\alpha_{oA(G184S:C351G)}$) in rat sympathetic neurons also reveals a prominent sigmoidal GIRK activation time course via $\alpha_2$-adrenergic receptor activation, and could be dramatically accelerated by coexpression of the N-terminal region of RGS8 (i.e. no RGS domain) (Jeong & Ikeda, 2001). The results of Jeong & Ikeda indicate the RGS8 N-terminal domain facilitates coupling of heterotrimeric $G\alpha_{oA(G184S:C351G)}\beta\gamma$ subunits to $\alpha_2$-adrenergic receptors, and as a consequence greatly accelerates the GIRK activation time course. Based on our observations of RGS7 reported here, we speculate that N-terminal regions of RGS7 may similarly interact with m2 receptors and facilitate coupling to $G\alpha_o$ in the absence of $G\beta5$.

### Physiological implications

GIRK channels mediate sIPSPs in the nervous system where the time course and amplitude of inhibitory synaptic events are dependent on the G protein cycle (Luscher *et al.* 1997). Thus RGS proteins are likely to play an important role in determining the amplitude and temporal properties of GIRK-mediated sIPSPs. Our findings demonstrate GIRK-mediated sIPSPs may be determined by specific GPCR–Gα–RGS signalling complexes that activate postsynaptic GIRK channels, where certain Gα–RGS precoupled complexes accelerate GIRK activation and deactivation kinetics without compromising amplitude. Perturbation of these signalling complexes would reduce inhibitory synaptic transmission and promote cellular excitability. The consequences of these events in the mammalian nervous system remain to be elucidated, yet the demonstrated role of RGS complexes in coordinating locomotion and egg laying behaviour in *Caenorhabditis elegans* highlight their potential impact on mammalian neural signalling (Chase *et al.* 2001; Robatzek *et al.* 2001).

## REFERENCES


Berman, D. M., Wilkie, T. M. & Gilman, A. G. (1996). GAIP and RGS4 are GTPase-activating proteins for the Gi subfamily of G protein α subunits. *Cell* **86**, 445–452.

Blake, B. L., Wing, M. R., Zhou, J. Y., Lei, Q., Hillmann, J. R., Behe, C. I., Morris, R. A., Harden, T. K., Bayliss, D. A., Miller, R. J. & Siderovski, D. P. (2001). Gβ association and effector interaction selectivities of the divergent Gγ subunit Gγ13. *Journal of Biological Chemistry* **276**, 49267–49274.

Breitwieser, G. E. & Szabo, G. (1988). Mechanism of muscarinic receptor-induced $K^+$ channel activation as revealed by hydrolysis-resistant GTP analogues. *Journal of General Physiology* **91**, 469–494.

Burgon, P. G., Lee, W. L., Nixon, A. B., Peralta, E. G. & Casey, P. J. (2001). Phosphorylation and nuclear translocation of a regulator of G protein signaling (RGS10). *Journal of Biological Chemistry* **276**, 32828–32834.

Chase, D. L., Patikoglou, G. A. & Koelle, M. R. (2001). Two RGS proteins that inhibit Gαo and Gαq signaling in *C. elegans* neurons require a Gβ5-like subunit for function. *Current Biology* **11**, 222–231.

Chen, C.-K., Wieland, T. & Simon, M. I. (1996). RGS-r, a retinal specific RGS protein, binds an intermediate conformation of transducin and enhances recycling. *Proceedings of the National Academy of Sciences of the USA* **93**, 12885–12889.

Corey, S. & Clapham, D. E. (2001). The stoichiometry of Gβγ binding to G-protein-regulated inwardly rectifying $K^+$ channels (GIRKs). *Journal of Biological Chemistry* **276**, 11409–11413.

Dascal, N. (1997). Signalling via the G protein-activated $K^+$ channels. *Cellular Signaling* **9**, 551–573.

Dascal, N., Schreibmayer, W., Lim, N. F., Wang, W., Chavkin, C., DiMagno, L., Labarca, C., Kieffer, B. L., Gaveriaux-Ruff, C., Trollinger, D., Lester, H. A. & Davidson, N. (1993). Atrial G protein-activated $K^+$ channel: Expression cloning and molecular properties. *Proceedings of the National Academy of Sciences of the USA* **90**, 10235–10239.

Destexhe, A. & Sejnowski, T. J. (1995). G protein activation kinetics and spillover of γ-aminobutyric acid may account for differences between inhibitory responses in the hippocampus and thalamus. *Proceedings of the National Academy of Sciences of the USA* **92**, 9515–9519.

Devic, E., Paquereau, L., Rizzoti, K., Monier, A., Knibiehler, B. & Audigier, Y. (1996). The mRNA encoding a β subunit of heterotrimeric GTP-binding proteins is localized to the animal pole of *Xenopus* laevis oocyte and embryos. *Mechanisms of Development* **59**, 141–151.

De Vries, L., Zheng, B., Fischer, T., Elenko, E. & Farquhar, M. G. (2000). The regulator of G protein signaling family. *Annual Review of Pharmacology and Toxicology* **40**, 235–271.

Dohlman, H. G., Song, J. P., Ma, D. R., Courchesne, W. E. & Thorner, J. (1996). SST2, a negative regulator of pheromone signalling in the yeast *Saccharomyces cerevisae* – expression, localization, and genetic interaction and physical association with GPA1 (the G-protein α-subunit). *Molecular and Cellular Biology* **16**, 5194–5209.

Dohlman, H. R., Apaniesk, D., Chen, Y., Song, J. P. & Nusskern, D. (1995). Inhibition of G-protein signaling by dominant gain-of-function mutations in Sst2p, a pheromone desensitization factor in *Saccharomyces cerevisae*. *Molecular and Cellular Biology* **15**, 3635–3643.

Doupnik, C. A., Davidson, N., Lester, H. A. & Kofuji, P. (1997). RGS proteins reconstitute the rapid gating kinetics of Gβγ-activated inwardly rectifying $K^+$ channels. *Proceedings of the National Academy of Sciences of the USA* **94**, 10461–10466.

Druey, K. M., Blumer, K. J., Kang, V. H. & Kehrl, J. H. (1996). Inhibition of G-protein-mediated MAP kinase activation by a new mammalian gene family. *Nature* **379**, 742–746.

Fernandez-Fernandez, J. M., Abogadie, F. C., Milligan, G., Delmas, P. & Brown, D. A. (2001). Multiple pertussis toxin-sensitive G-proteins can couple receptors to GIRK channels in rat sympathetic neurons when expressed heterologously, but only native $G_i$-proteins do so in situ. *European Journal of Neuroscience* **14**, 283–292.

Fernandez-Fernandez, J. M., Wanaverbecq, N., Halley, P., Caulfield, M. P. & Brown, D. A. (1999). Selective activation of heterologously expressed G protein-gated $K^+$ channels by M2 muscarinic receptors in rat sympathetic neurones. *Journal of Physiology* **515**, 631–637.

Granneman, J. G., Zhai, Y., Zhu, Z., Bannon, M. J., Burchett, S. A., Schmidt, C. J., Andrade, R. & Cooper, J. (1998). Molecular characterization of human and rat RGS 9L, a novel splice variant enriched in dopamine target regions, and chromosomal localization of the RGS 9 gene. *Molecular Pharmacology* **54**, 687–694.

Greif, G. J., Sodickson, D. L., Bean, B. P., Neer, E. J. & Mende, U. (2000). Altered regulation of potassium and calcium channels by $GABA_B$ and adenosine receptors in hippocampal neurons from mice lacking Gαo. *Journal of Neurophysiology* **83**, 1010–1018.

Henry, D. J., Grandy, D., Lester, H. A., Davidson, N., Lim, N. F. & Chavkin, C. (1995). κ opioid receptors couple to inwardly rectifying potassium channels when coexpressed in *Xenopus* oocytes. *Molecular Pharmacology* **47**, 551–557.

Herlitze, S., Ruppersberg, J. P. & Mark, M. D. (1999). New roles for RGS2, 5 and 8 on the ratio-dependent modulation of recombinant GIRK channels expressed in *Xenopus* oocytes. *Journal of Physiology* **517**, 341–352.

Hodgkin, A. L. & Huxley, A. F. (1952). A quantitative description of membrane current and its application to conduction and excitation in nerve. *Journal of Physiology* **117**, 500–544.

Hosoya, Y., Yamada, M., Ito, H. & Kurachi, Y. (1996). A functional model for G protein activation of the muscarinic $K^+$ channel in guinea pig atrial myocytes. Spectral analysis of the effect of GTP on single-channel kinetics. *Journal of General Physiology* **108**, 485–495.

Huang, C.-L., Slesinger, P. A., Casey, P. J., Jan, Y. N. & Jan, L. Y. (1995). Evidence that direct binding of Gβγ to the GIRK1 G protein-gated inwardly rectifying $K^+$ channel is important for channel activation. *Neuron* **15**, 1133–1143.

Hunt, T. W., Fields, T. A., Casey, P. J. & Peralta, E. G. (1996). RGS10 is a selective activator of Gαi GTPase activity. *Nature* **383**, 175–177.

Inanobe, A., Fujita, S., Makino, Y., Matsushita, K., Ishii, M., Chachin, M. & Kurachi, Y. (2001). Interaction between the RGS domain of RGS4 with G protein α subunits mediates the voltage-dependent relaxation of the G protein-gated potassium channel. *Journal of Physiology* **535**, 133–143.

Inomata, N., Ishihara, T. & Akaike, N. (1989). Activation kinetics of the acetylcholine-gated potassium current in isolated atrial cells. *American Journal of Physiology* **257**, C646–650.

Ivanova-Nikolova, T. T., Nikolov, E. N., Hansen, C. & Robishaw, J. D. (1998). Muscarinic $K^+$ channel in the heart. Modal regulation by G protein βγ subunits. *Journal of General Physiology* **112**, 199–210.

Jeong, S. W. & Ikeda, S. R. (1999). Sequestration of G-protein βγ subunits by different G-protein α subunits blocks voltage-dependent modulation of $Ca^{2+}$ channels in rat sympathetic neurons. *Journal of Neuroscience* **19**, 4755–4761.

Jeong, S. W. & Ikeda, S. R. (2001). Differential regulation of G protein-gated inwardly rectifying $K^+$ channel kinetics by distinct domains of RGS8. *Journal of Physiology* **535**, 335–347.

Keren-Raifman, T., Bera, A. K., Zveig, D., Peleg, S., Witherow, D. S., Slepak, V. Z. & Dascal, N. (2001). Expression levels of RGS7 and RGS4 proteins determine the mode of regulation of the G protein-activated $K^+$ channel and control regulation of RGS7 by Gβ5. *FEBS Letters* **492**, 20–28.

Koelle, M. R. & Horvitz, H. R. (1996). EGL-10 regulates G protein signaling in the *C. elegans* nervous system and shares a conserved domain with mammalian proteins. *Cell* **84**, 115–125.

Kovoor, A., Chen, C. K., He, W., Wensel, T. G., Simon, M. I. & Lester, H. A. (2000). Co-expression of Gβ5 enhances the function of two Gγ subunit-like domain-containing regulators of G protein signaling proteins. *Journal of Biological Chemistry* **275**, 3397–3402.

Kovoor, A. & Lester, H. A. (2002). Gi Irks GIRKs. *Neuron* **33**, 6–8.

Krapivinsky, G., Krapivinsky, L., Wickman, K. & Clapham, D. E. (1995). Gβγ binds directly to the G protein-gated $K^+$ channel, IKACh. *Journal of Biological Chemistry* **270**, 29059–29062.

Lan, K. L., Zhong, H., Nanamori, M. & Neubig, R. R. (2000). Rapid kinetics of Regulator of G-protein Signaling (RGS)-mediated Gαi and Gαo deactivation: Gα specificity of RGS4 and RGS7. *Journal of Biological Chemistry* **275**, 33497–33503.

Leaney, J. L., Milligan, G. & Tinker, A. (2000). The G protein α subunit has a key role in determining the specificity of coupling to, but not the activation of, G protein-gated inwardly rectifying $K^+$ channels. *Journal of Biological Chemistry* **275**, 921–929.

Leaney, J. L. & Tinker, A. (2000). The role of members of the pertussis toxin-sensitive family of G proteins in coupling receptors to the activation of the G protein-gated inwardly rectifying potassium channel. *Proceedings of the National Academy of Sciences of the USA* **97**, 5651–5656.

Lei, Q., Jones, M. B., Talley, E. M., Schrier, A. D., McIntire, W. E., Garrison, J. C. & Bayliss, D. A. (2000). Activation and inhibition of G protein-coupled inwardly rectifying potassium (Kir3) channels by G protein βγ subunits. *Proceedings of the National Academy of Sciences of the USA* **97**, 9771–9776.

Levay, K., Cabrera, J. L., Satpaev, D. K. & Slepak, V. Z. (1999). Gβ5 prevents the RGS7-Gαo interaction through binding to a distinct Gγ-like domain found in RGS7 and other RGS proteins. *Proceedings of the National Academy of Sciences of the USA* **96**, 2503–2507.

Li, Y., Mende, U., Lewis, C. & Neer, E. J. (1996). Maintenance of cellular levels of G-proteins: different efficiencies of αs and αo synthesis in GH3 cells. *Biochemistry Journal* **318**, 1071–1077.

Lim, N. F., Dascal, N., Labarca, C., Davidson, N. & Lester, H. A. (1995). A G protein-gated K channel is activated via β2-adrenergic receptors and Gβγ subunits in *Xenopus* oocytes. *Journal of General Physiology* **105**, 421–439.

Liman, E. R., Tytgat, J. & Hess, P. (1992). Subunit stoichiometry of a mammalian $K^+$ channel determined by construction of multimeric cDNAs. *Neuron* **9**, 861–871.

Lledo, P. M., Homburger, V., Bockaert, J. & Vincent, J. D. (1992). Differential G protein-mediated coupling of D2 dopamine receptors to $K^+$ and $Ca^{2+}$ currents in rat anterior pituitary cells. *Neuron* **8**, 455–463.

Logothetis, D. E., Kurachi, Y., Golper, J., Neer, E. J. & Clapham, D. (1987). The βγ-subunit of GTP-binding proteins activate the muscarinic $K^+$ channel in heart. *Nature* **325**, 321–326.

Luscher, C., Jan, L. Y., Stoffel, M., Malenka, R. C. & Nicoll, R. A. (1997). G protein-coupled inwardly rectifying $K^+$ channels (GIRKs) mediate postsynaptic but not presynaptic transmitter actions in hippocampal neurons. *Neuron* **19**, 687–695.

Mark, M. D. & Herlitze, S. (2000). G-protein mediated gating of inward-rectifier $K^+$ channels. *European Journal of Biochemistry* **267**, 5830–5836.

Nemec, J., Wickman, K. & Clapham, D. E. (1999). Gβγ binding increases the open time of IKACh: kinetic evidence for multiple Gβγ binding sites. *Biophysical Journal* **76**, 246–252.

Posner, B. A., Gilman, A. G. & Harris, B. A. (1999). Regulators of G protein signaling 6 and 7. Purification of complexes with Gβ5 and assessment of their effects on G protein-mediated signaling pathways. *Journal of Biological Chemistry* **274**, 31087–31093.

Robatzek, M., Niacaris, T., Steger, K., Avery, L. & Thomas, J. H. (2001). Eat-11 encodes GPB-2, a Gβ5 ortholog that interacts with Goα and Gqα to regulate *C. elegans* behavior. *Current Biology* **11**, 288–293.

Rose, J. J., Taylor, J. B., Shi, J., Cockett, M. I., Jones, P. G. & Hepler, J. R. (2000). RGS7 is palmitoylated and exists as biochemically distinct forms. *Journal of Neurochemistry* **75**, 2103–2112.

Ross, E. M. & Wilkie, T. M. (2000). GTPase-activating proteins for heterotrimeric G proteins: Regulators of G Protein Signaling (RGS) and RGS-like proteins. *Annual Review of Biochemistry* **69**, 795–827.

Saitoh, O., Kubo, Y., Miyatani, Y., Asano, T. & Nakata, H. (1997). RGS8 accelerates G-protein-mediated modulation of $K^+$ currents. *Nature* **390**, 525–529.

Saitoh, O., Kubo, Y., Odagiri, M., Ichikawa, M., Yamagata, K. & Sekine, T. (1999). RGS7 and RGS8 differentially accelerate G protein-mediated modulation of $K^+$ currents. *Journal of Biological Chemistry* **274**, 9899–9904.

Saitoh, O., Odagiri, M., Masuho, I., Nomoto, S. & Kinoshita, N. (2000). Molecular cloning and characterization of *Xenopus* RGS5. *Biochemical and Biophysical Research Communications* **270**, 34–39.

Schreibmayer, W., Dessauer, C. W., Vorobiov, D., Gilman, A. G., Lester, H. A., Davidson, N. & Dascal, N. (1996). Inhibition of an inwardly rectifying $K^+$ channel by G-protein α-subunits. *Nature* **380**, 624–627.

Shea, L. & Linderman, J. J. (1997). Mechanistic model of G-protein signal transduction. Determinants of efficacy and effect of precoupled receptors. *Biochemical Pharmacology* **53**, 519–530.

Shea, L. D., Neubig, R. R. & Linderman, J. J. (2000). Timing is everything: the role of kinetics in G protein activation. *Life Sciences* **68**, 647–658.

Simon, M. I., Strathmann, M. P. & Gautam, N. (1991). Diversity of G proteins in signal transduction. *Science* **252**, 802–808.

Slesinger, P. A., Reuveny, E., Jan, Y. N. & Jan, L. Y. (1995). Identification of structural elements involved in G protein gating of the GIRK1 potassium channel. *Neuron* **15**, 1145–1156.

Snow, B. E., Krumins, A. M., Brothers, G. M., Lee, S. F., Wall, M. A., Chung, S., Mangion, J., Arya, S., Gilman, A. G. & Siderovski, D. P. (1998). A G protein γ subunit-like domain shared between RGS11 and other RGS proteins specifies binding to Gβ5 subunits. *Proceedings of the National Academy of Sciences of the USA* **95**, 13307–13312.

Sodickson, D. L. & Bean, B. P. (1996). $GABA_B$ receptor-activated inwardly rectifying potassium current in dissociated hippocampal CA3 neurons. *Journal of Neuroscience* **16**, 6374–6385.

Sondek, J. & Siderovski, D. P. (2001). Gγ-like (GGL) domains: new frontiers in G-protein signaling and β-propeller scaffolding. *Biochemical Pharmacology* **61**, 1329–1337.

Sowell, M. O., Ye, C., Ricupero, D. A., Hansen, S., Quinn, S. J., Vassilev, P. M. & Mortensen, R. M. (1997). Targeted inactivation of αi2 or αi3 disrupts activation of the cardiac muscarinic $K^+$ channel, IKACh, in intact cells. *Proceedings of the National Academy of Sciences of the USA* **94**, 7921–7926.

Stuhmer, W. & Parekh, A. B. (1995). Electrophysiological recordings from *Xenopus* oocytes. In *Single-Channel Recording*, ed. Sakmann, B. & Neher, E., pp. 341–356. Plenum Press, New York.

Takano, K., Yasufuku-Takano, J., Kozasa, T., Nakajima, S. & Nakajima, Y. (1997). Different G proteins mediate somatostatin-induced inward rectifier $K^+$ currents in murine brain and endocrine cells. *Journal of Physiology* **502**, 559–567.

Valenzuela, D., Han, X., Mende, U., Fankhauser, C., Mashimo, H., Huang, P., Pfeffer, J., Neer, E. J. & Fishman, M. C. (1997). Gαo is necessary for muscarinic regulation of $Ca^{2+}$ channels in mouse heart. *Proceedings of the National Academy of Sciences of the USA* **94**, 1727–1732.

Vivaudou, M., Chan, K. W., Sui, J. L., Jan, L. Y., Reuveny, E. & Logothetis, D. E. (1997). Probing the G-protein regulation of GIRK1 and GIRK4, the two subunits of the KACh channel, using functional homomeric mutants. *Journal of Biological Chemistry* **272**, 31553–31560.

Watson, N., Linder, M. E., Druey, K. M., Kehrl, J. H. & Blumer, K. J. (1996). RGS family members: GTPase-activating proteins for heterotrimeric G-protein α-subunits. *Nature* **383**, 172–177.

Wickman, K. D., Inlguez-Lluhl, J. A., Davenport, P. A., Taussig, R., Krapivinsky, G. B., Linder, M. E., Gilman, A. G. & Clapham, D. E. (1994). Recombinant G-protein βγ-subunits activate the muscarinic-gated atrial potassium channel. *Nature* **368**, 255–257.

Wise, A., Watson-Koken, M. A., Rees, S., Lee, M. & Milligan, G. (1997). Interactions of the α2A-adrenoceptor with multiple Gi-family G-proteins: studies with pertussis toxin-resistant G-protein mutants. *Biochemistry Journal* **321**, 721–728.

Yamada, M., Inanobe, A. & Kurachi, Y. (1998). G protein regulation of potassium ion channels. *Pharmacological Reviews* **50**, 723–760.

Yu, J. H., Wieser, J. & Adams, T. H. (1996). The *Aspergillus* FlbA RGS domain protein antagonizes G protein signaling to block proliferation and allow development. *EMBO Journal* **15**, 5184–5190.

Zerangue, N. & Jan, L. Y. (1998). G-protein signaling: fine-tuning signaling kinetics. *Current Biology* **8**, R313–316.

**Acknowledgements**

We thank the following colleagues for generously providing cDNAs used in this study: Stephen Ikeda, NIAAA/NIH (PTX-insensitive $G\alpha_{i/o}$ subunits); Henry Lester, Caltech (Kir3.1, Kir3.2a, m2 receptor, RGS4), Vlad Slepak, University of Miami (RGS7 and Gβ 5); and Eitan Reuveny, Weizmann Institute of Science (PTX-S1 subunit). The authors also thank Ms Jenny Gulledge for technical assistance. This work was supported by an Initial Investigator Award (C.D.) and a Women and Minorities Award (M.P.) from the American Heart Association (Florida-Puerto Rico Affiliate), and a Research and Creative Scholarship Award from the University of South Florida (C.D.).